République Algérienne Démocratique et Populaire
Ministère de l'Enseignement Superieure et de la Recherche Scientifique

Université Echahid Hamma Lakhdar d'El-Oued
FACULTE DE TECHNOLOGIE
DEPARTEMENT DE GENIE MECANIQUE

Présenté pour l'obtention du diplôme de

MASTER ACADEMIQUE

Domaine: Sciences et Technologie
Filière: Génie mécanique
Spécialité: Energétique

Thème

Bi-dimensional modeling and simulation of thermo-fluidic behavior in low temperature fuel cell system

Présenté par

ZOBIRI Oussama

BEGGAT Ridha

Devant le jury composé de

KHECHANA Mohammed	MCA	Président	UEHL El-Oued
ZINE Bachir	MCB	Examinateur	UEHL El-Oued
ATIA Abdelmalek	MCA	Encadreur	UEHL El-Oued

2017-2018

Résumé

A cause de la crise énergétique et l'augmentation du niveau de pollution à travers le monde, une nouvelle source d'énergie propre est la pile à combustible. Le PEMFC (pile à combustible à membrane échangeuse de protons) est type de pile le plus étudié. Dans notre sujet, on s'intéresse à la modélisation et simulation des écoulements de dans la couche diffuseur de gaz (Gaz Diffusion Layer « GDL ») a l'aide de la méthode de Boltzmann sur réseau. Le modèle D_2Q_9de la méthode LBM a été choisi pour étudier l'influence des différents paramètres physique sur l'écoulement de gaz dans le milieu poreux de GDL tels que la perméabilité, la porosité la vitesse d'enter. Les résultats trouvés montrent que tous ces paramètres à influences sur la morphologie de l'écoulement et par conséquent sur les performances de la pile. D'aideur, les résultats montrent aussi que la méthode de Boltzmann sur réseau peut produire des prédictions efficaces sur les phénomènes physiques qui se produisent dans le GDL qui peut utiliser pour améliorer la productivité de la PEMFC

Mots clés : Pile à combustible, Modélisation, Simulation, Boltzmann sur réseau.

Abstract :

Due to the energy crisis and the rising level of pollution around the world, a new source of clean energy is the fuel cell. PEMFC (Proton Exchange Membrane Fuel Cell) is the most studied type of cell. In our subject, we are interested in the modeling and simulation of flows in gas diffusion layer ("GDL") using the lattice Boltzmann method. The D_2Q_9 model of the LBM method was chosen to study the influence of different physical parameters on gas flow in the porous GDL medium such as permeability, porosity and inlet velocity. The results found show that all these parameters have an influence on the morphology of the flow and as consequently the performance of the full cells. In other side, the results also show that the lattice Boltzmann method can produce efficient predictions about the physical phenomena that occur in the GDL that can use to improve the productivity of the PEMFC

Key words: Fuel cell; Modeling; Simulation; Lattice Boltzmann Method.

ملخص:

بسبب أزمة الطاقة وارتفاع مستوى التلوث حول العالم ، فإن مصدرًا جديدًا للطاقة النظيفة هو خلية الوقود PEMFC. (خلية وقود غشاء التبادل البروتوني) هي أكثر أنواع الخلايا التي تمت دراستها .في موضوعنا ، نحن مهتمون في النمذجة والمحاكاة من طبقة الانتشار الغاز التدفقات ("GDL") باستخدام طريقة بولتزمان شعرية .تم اختيار نموذج D_2Q_9 لطريقة LBMلدراسة تأثير العوامل الفيزيائية المختلفة على تدفق الغاز في وسط GDL المسامي مثل النفاذية والمسامية وسرعة الدخول .تظهر النتائج التي تم العثور عليها أن جميع هذه المعلمات لها تأثير على مورفولوجيا التدفق وبالتالي على أداء الخلايا الكاملة .في الجانب الآخر ، تظهر النتائج أيضًا أن طريقة بولتزمان الشبكية يمكن أن تنتج توقعات فعالة حول الظواهر الفيزيائية التي تحدث في GDL والتي يمكن استخدامها لتحسين إنتاجيةPEMFC

الكلمات المفتاحية : خلية وقود , النمذجة, المحاكاة ، طريقة بولتزمان الشبكية.

Dedication

To our parents,

To our families,

To our friends

Thankfulness

*First of all, we thank **ALLAH**, our creator for giving us the strength to do this work. We send a big thank to our supervisor Dr. **ATIA Abdelmalek** who proposed this work also for his useful advice and guidance.*

We also have the honor to thank all staff of Mechanical Engineering Department for their useful work, information organization and coordination.

Many thanks to the reviewers of this thesis, for accepting, reading and evaluation of our work.
Finally, we thank all those who participated in making this thesis.

Table of contents

Chapter III :Numerical simulation and results discussion

List of figures

List of tables

Nomenclature

η_{HHV} the theoretical fuel cell efficiency
j,I_{fc} the fuel cell current A/m^2
V_{op},V_{fc} the generated voltage ,V
ΔH_{HHV} Higher Heating Value of hydrogen
F_{ar} Faraday constant, 96487 C/mol
P_{fc} the fuel cell power ,W
P_{H2} hydrogen power ,W
P_{net} the net power output ,W
P_{aux} the power consumed ,W
η_{fc} the efficiency of the fuel cell system
p_{O2} partial pressures of oxygen ,atm
p_{H2} partial pressures of hydrogen ,atm
T Temperature, K
C Concentration of gas
c Lattice velocity set to unity
x Position vector, m
c_i Discrete velocity vector
D_e Effective diffusion coefficient of gaz , $m^2 \cdot s^{-1}$
D Diffusion coefficient of gas , $m^2 \cdot s^{-1}$
f_i Density distribution function
f_i^{eq} Equilibrium distribution function
T_i Temperature distribution function
T_i^{eq} Equilibrium distribution function of the temperature
C_i Concentration distribution function
C_i^{eq} Equilibrium distribution function of Concentration
υ Kinematic viscosity, $m^2.s^{-1}$
υ_e Effective kinematic viscosity, $m^2.s^{-1}$
ε Porosity
τ_{sub} Dimensionless relaxation time
λ Thermal conductivity, W/m K
λ_e Effective thermal conductivity, W/m K
c_p Thermal capacity , J/(kg K)
dt,δt Lattice time step size
dx,δx Lattice space step size
Δx Space interval
Δt Time interval
α_e Effective thermal diffusivity
σ Specific heat ratio
μ Dynamic viscosity, Pa.s
ω_i Weight factor

α_a Anodic transfer coefficient, 0.5

E, U_0 thermodynamic equilibrium potential, V

$j_{0,a}^{ref}$ reference exchange current density, A/m^2

ρ Macroscopic density , $kg.m^{-3}$

F The total body force

G the external body force

R Universal gas constant, 8.314 J/mol K

k Permeability

v,u The fluid velocity, m/s

Subscripts

eq Equilibrium

f fluid

s solid

e Effective

Abbreviations

LBM Lattice Boltzmann Method

GDL Gas Diffusion Layer

CL Catalyst Layer

MEA Membrane Electrode Assembly

ORR Oxygen Reduction Reaction

HOR Hydrogen Oxidation Reaction

Fig Figure

General introduction

General introduction

Currently, the energy crisis and the rising level of pollution are major problems around the world. New, renewable and clean sources of energy must therefore be considered. A possible new source is the fuel cell, the principle of which was discovered by Sir William Grove in 1839 [1].

A fuel cell uses the chemical energy of hydrogen and oxygen to produce electricity without pollution. Other products are simply pure water and heat. Scientists have already and continue to develop different types of fuel cells, characterized by the nature of the gases and the electrolyte used, thus determining its operating characteristics. A promising type, lightweight and easy to build, is the polymer electrolyte membrane cell (PEMFC), used by NASA in the 1960's in the Gemini space program [2] .

As far as our work is concerned, we are interested in a proton exchange membrane (PEM) fuel cell. The latter is currently considered to be the most suitable for the automotive sector. Its strengths are a relatively fast dynamic compared to other types of batteries and a low operating temperature of 40 to 100 ° C which facilitates its integration into a vehicle without specific thermal insulation.

Object this work to study thermo-fluidic behavior of the fluid in anodic layer (porous medium) using the Lattice Boltzmann Method (LBM).

This thesis is presented in the form of three chapters:

Chapter I presented a general introduction to fuel cells and their applications. As the PEMFC cell is the subject of this study, a detailed description of each element constituting a cell makes it possible to specify the composition of a cell core as well as electrochemical processes.

Chapter II provides an introduction to the chosen computational methodology, the Lattice Boltzmann Method (LBM). In this chapter, we will introduce the methodology and general concepts of LB method.

Chapter III presents a numerical simulation study relative to the effect of different parameters such permeability, porosity on the mechanism of gas flow. The numerical scheme employed for this study is based on Lattice Boltzmann Method (LBM) for fluid flow and mass transfer in porous media.

CHAPTER I:State of art on PEM Fuel Cells

I.1 Introduction

Proton Exchange Membrane Fuel Cells (PEM Fuel cells) offer the capability to provide clean energy transportation with zero tailpipe carbon dioxide (CO2) emissions. Even where their fuel must be sourced from fossil fuels, the high efficiency of fuel cells relative to internal combustion engines still offers the potential for reduced well to wheel CO2 emissions . PEMFCs have dominated the transportation fuel cell market and will do so for the foreseeable future for several reasons .

Fuel cells used pure oxygen and pure hydrogen and were small, expensive and not commercially available. NASA's interest in fuel cells and the 1973 energy crisis revived the development of this device. Since then, fuel cell research has continued and fuel cells have been used successfully in a wide variety of applications.

I.2 Definition

Fuel cell can be defined as a device that converts chemical energy into electrical energy in a controlled reaction. The fuel cell has often been compared with a battery, the different being that while the reactants and electrolyte in a battery is sealed into the battery the fuel cell is supplied with fresh reactants. These reactants were being referred to as fuels[3].

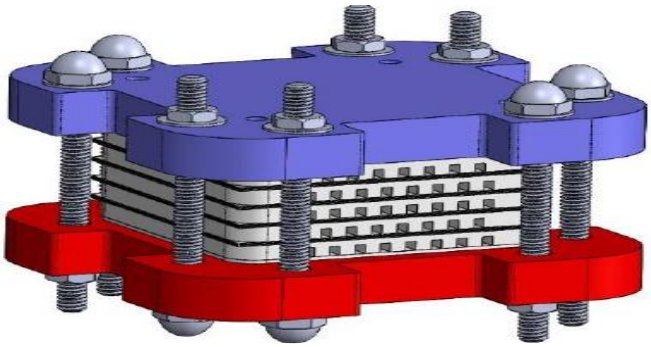

Fig I.1: Schematic of fuel cells[3]

I.3 The operating principle

The operating principle of the fuel cell is quite old. This principle was introduced by two researchers (Christian Friedrich Schönberg and William Grove) within a span of one month in 1839. The principle is based on the reaction between two gases: hydrogen (or a hydrogen-rich gas) used as fuel and oxygen used as oxidant. The operating principle of the fuel cell is relatively straightforward: it can be described as inverse electrolysis. More precisely, it consists of a controlled electrochemical combustion between oxygen and hydrogen resulting in the simultaneous production of electricity, water, and heat, following the global formula:

$$\text{Hydrogen} + \text{Oxygen (from air)} \Rightarrow \text{Electricity} + \text{Water} + \text{Heat} \quad \text{(I.1)}$$

This electrochemical reaction takes place in a system which consists of two electrodes (cathode and anode) separated by an electrolyte. Depending on the type of the fuel cell, the reaction can take place at different temperatures, from a few dozens of degrees Celsius for proton exchange membrane fuel cells[4]

the operating principle of proton exchange membrane fuel cells is shown in Fig.I.2

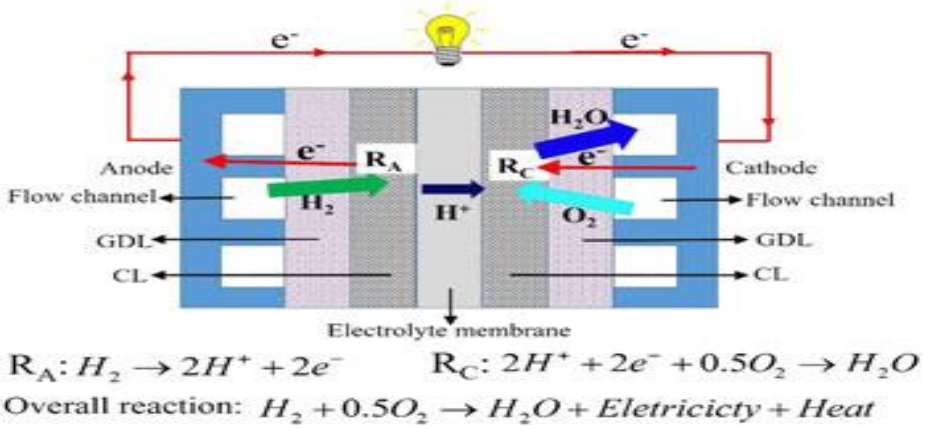

Fig I.2: Schematic of proton exchange membrane fuel cell[4]

I.4 Fuel (hydrogen)

Pure hydrogen is usually the preferred fuel because it is the one that allows the highest power densities per active cell surface . Hydrogen is the most abundant element in the universe. It makes up 75% of the mass of all matter in stars and galaxies. A hydrogen atom has only one proton and one electron. However, hydrogen gas (H_2) does not exist naturally on earth and is in compound forms. Combined with oxygen, it is water (H_2O). Combined with carbon, it forms organic compounds such as methane (CH_4), coal or oil.

Most of the energy we use today comes from fossil fuels. Only seven percent come from renewable energy sources. With a view to reducing fossil fuels, hydrogen appears to be a promising energy carrier. Since hydrogen gas does not exist naturally on earth, it must be produced [5] .

There are several ways to do this. If hydrogen is produced from the electrolysis of water, the electrolyser being fed from a renewable energy source (solar panel, wind turbine or hydroelectric turbine), there will be no carbon dioxide emissions[6] . The development of fuel cells will lead to different modes of production linked to local methods of energy production.

Due to the abundance of natural gas, the availability of methanol and propane, and the lack of a hydrogen generation and distribution infrastructure, it is expected that hydrocarbon fuels will be the dominant fuels for stationary applications. of fuel cells. As long as these fuels are available at low cost, hydrocarbon reforming is the simplest and most efficient method for producing hydrogen [7] .

I.5 PEM fuel cells structure

A single PEM fuel cell consist of seven components, according to Fig I.3 [8]: feeding channels, diffusion layer, and catalytic layer in the anode; membrane; catalytic layer, diffusion layer, and feeding channels in the cathode. The PEMFC combines in a very compact

unit the electrodes and the electrolyte .This structure, well known as membrane electrode assembly (MEA)

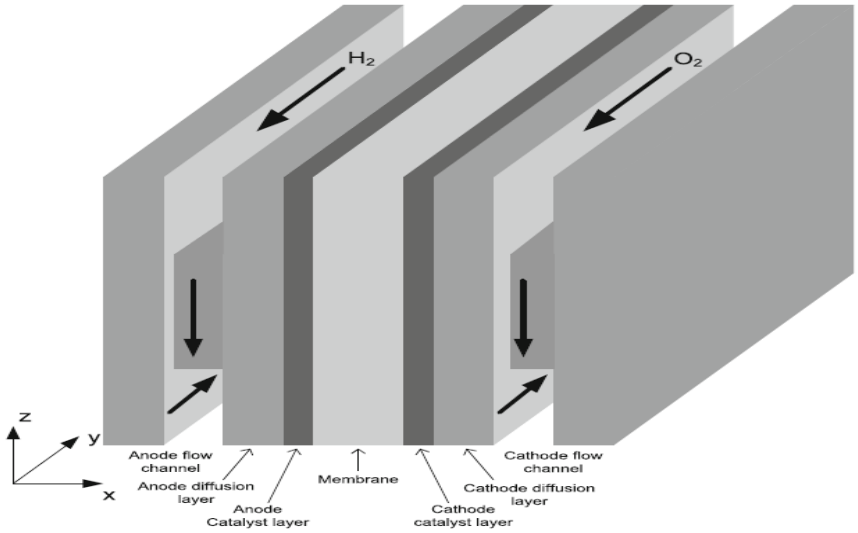

Fig I.3:Three-dimensional schematic of a fuel cell[8]

I.5.1 Bipolar plates

Bipolar plates form the border between two elementary fuel cells in a stack, and play an important role in their mechanical structure support.

Graphite was one of the first materials used to make bipolar plates, since it had shown excellent stability under fuel cell operating conditions (high temperature, corrosion). However, on the plate's surface, micro channels would be required for gas supply that could take many configurations (parallel, serpentine, grill, parallel-serpentine, etc.) Fig I.4. The costs of channel machining on graphite plate are often too high for mass production and commercialization of fuel cells. In addition, since graphite is naturally porous, the plates require specific treatments to render them impervious to gas (reactants).

Metallic plates have a major drawback as compared to graphite [9]: whether based on aluminum, titanium or nickel, they are subject to corrosion (due to weak pH, between 2 and 3, and high temperature). A plate's corrosion results in membrane poisoning (diffusion of the metallic ions) and increases electrical contact resistance of the bipolar plate. For this reason, metallic plates must be coated with a layer of non-corrosive material (graphite, noble metals, conductive polymers, etc.) which also needs to be electrically conductive.

They have many roles[10]:

– feeding reactants (hydrogen, oxygen or air from either side of the plate) through the channels to the diffusion layers;

– providing the fuel cells' mechanical support. The cell must resist mechanical constraints (clamping force) while remaining as light as possible so as to increase the fuel cells' power density (specific power);

-evacuating heat from the electrochemical reaction towards the cooling channels. The plates' thermal conductivity must be as high as possible: if the plate is cooled by a fluid, it must be at least 20 W/m K and greater than 100 W/m K when the heat is evacuated through the plate alone;

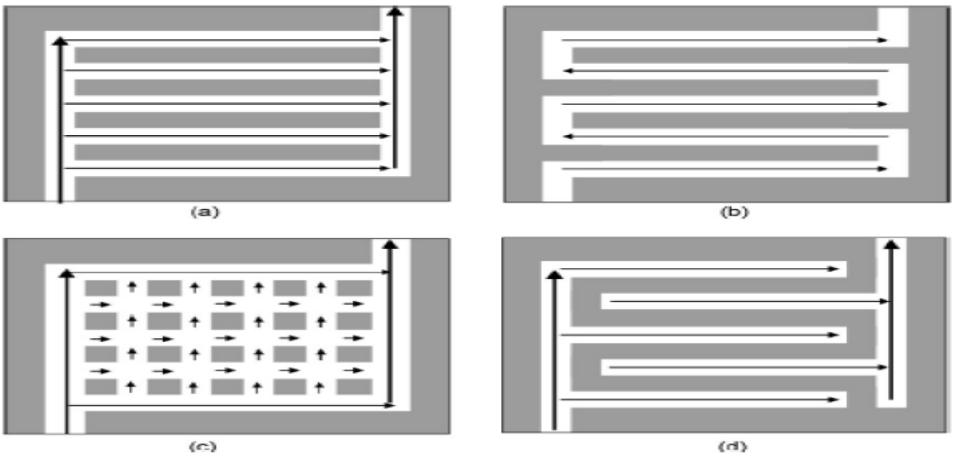

Fig I.4 : Most used channel patterns: a) Parallel channels, b) Serpentine channels, c) Pine channels, d) Interdigit channels[11]

I.5.2 Membrane Electrode Assembly

I.5.2.1Types of assembly

Fundamentally there are two fabrication methods to assemble the MEA for PEMFC and are distinguished on the basis on where the catalyst ink is deposited to make the electrode. The first method is by deposition of the catalyst layer on a porous GDL such as carbon paper, followed by hot pressing it with the membrane to make the membrane. This method is commonly known as catalyst-coated substrate (CCS). In the second method, the catalyst layer is deposited directly onto the membrane; this method is referred to as catalyst-coated membrane (CCM)[3]. Fig I.5 illustrates the two methods.

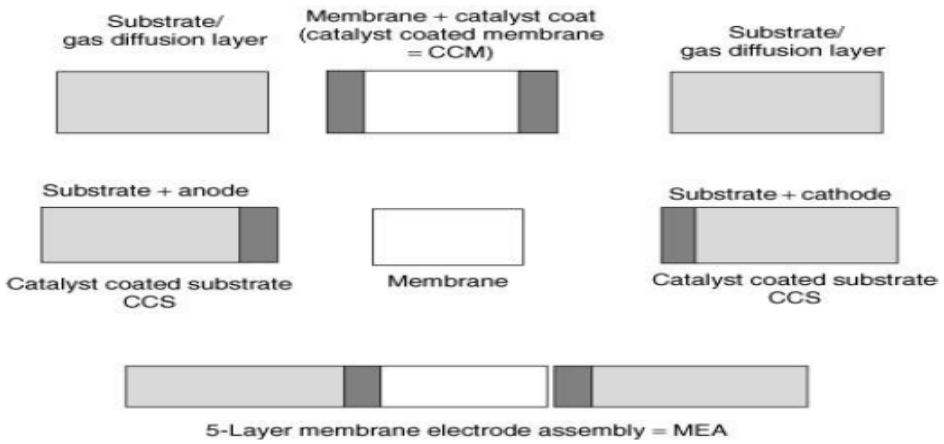

Fig I.5: MEA's CCM and CCS[3]

I.5.2.2 Electrodes

Reactions that involve oxidation of hydrogen and reduction of oxygen take place at the electrodes. These electrodes consist of a carbon paper or cloth, where the surface in contact with the electrolyte is coated with a hydrophobic polymer and platinum-carbon particles (catalyst).

Two zones can be distinguished in these electrodes:

– the porous diffusion layer, which ensures the reactant gas supply to catalyst sites and evacuation of byproducts;

– the active zone with catalyst particles, which is where the electrochemical reactions take place.

The diffusion layer should be designed in a manner that multiple goals can be achieved:

– being a good electrical conductor to enable the transport of electrons to the bipolar plates;

– being a good thermal conductor to enable the evacuation of heat from the reaction sites toward the cooling channels in the bipolar plates;

– ensuring the efficient diffusion of the reactants (oxygen or hydrogen) from the channels to the active zone so as to minimize the fuel cell's concentration losses. The material used must be porous enough to carry this function out (porosity can vary between 40% and 80% in diffusion layer [12]);

In addition to the diffusion layer, the active zone, or catalyst layer, is where electrochemical reactions occur. Reactions take place in the triple contact zone (electrolyte, catalyst and reactants), and the interface between the diffusion layer and the electrolyte membrane .

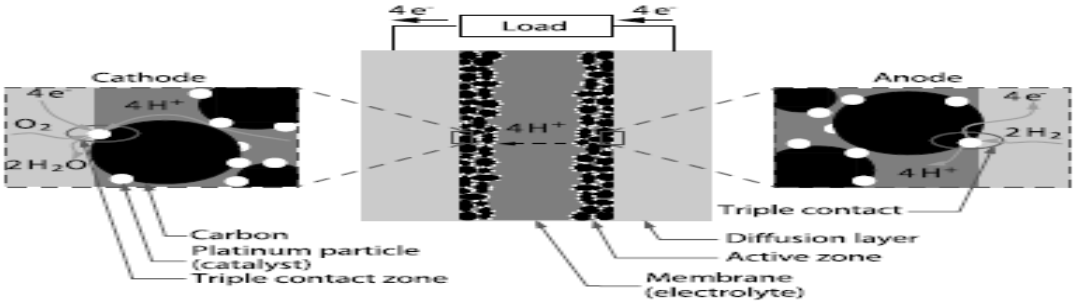

Fig I.6:Anodic and Cathodic triple contact zones[12]

Platinum is the most commonly used catalyst for the reduction of oxygen at the cathode and the oxidation of hydrogen at the anode. Using a catalyst enables us to increase the reaction rate of a given chemical reaction. With the presence of platinum, the rate of oxygen reduction at the cathode and hydrogen oxidation at the anode is increased tenfold [10].

There are four main characteristics that are essential for an effective PEMFC catalyst:

(a) Activity – to be able to adsorb the reactant strongly enough to facilitate a reaction but not so strongly that the catalyst becomes blocked by the reactant or products.

(b) Selectivity – to make the desired product and minimise the production of undesirable intermediates and side products.

(c) Stability – to withstand the operating environment in a fuel cell, including strong oxidants, reactive radicals, an acidic environment and high and rapidly fluctuating temperatures, all whilst under an applied voltage.

(d) Poisoning resistance – to be resistant to poisoning by impurities likely to be found in the fuel cell itself and in the feed gases.

I.5.2.3 Membrane

The electrolyte is placed between the cathodic and anodic active zones of the electrodes. The electrolyte in a proton exchange membrane fuel cell is a solid polymer membrane designed to:

1) Conduct protons from the anode to the cathode with as few ohm losses as possible. The membrane must have as high proton conductivity as possible: the thinner the membrane, the higher the protonic conductance.

2) Electrically isolate the cathodic and anodic electrodes.

3) Separate the cathodic (oxygen) and anodic (hydrogen) reactants on either side of the membrane so as to avoid any direct reactions between the two, since such a reaction would be destructive to the fuel cell. Impermeability of the gas increases with membrane thickness.

Membrane conductivity also depends on temperature, which can vary between 25◦C and 80◦C under normal operating conditions. The higher the temperature, the higher the ionic conductivity and the better the fuel cell performance. Thus, increasing the temperature from 25◦C to 80◦C doubles the membrane's conductivity [13]. The most widespread membrane is Nafion®, whose formula is given in Fig.I.7

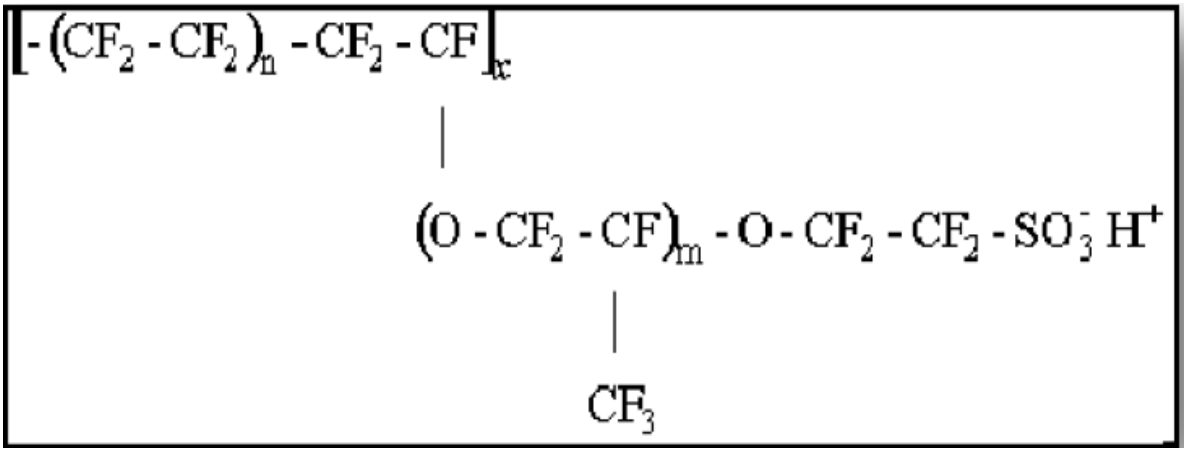

Fig I.7 : Chemical formula of Nafion®[13]

I.6 Electrochemical processes [14]

I.6.1 Anode Processes

Hydrogen flows into the fuel cell and reaches the Pt anode where the HOR takes place. Here the hydrogen adsorbs onto the surface of the Pt electrode, breaking the hydrogen–hydrogen bond to give adsorbed atomic hydrogen (H*)

$$\tfrac{1}{2}\, H_2 + * \rightarrow H^* \qquad \text{(I.2)}$$

(where * denotes a surface site). Subsequent loss of an electron from each adsorbed hydrogen leads to hydrogen leaving the surface as protons (H^+)

$$H^* \rightarrow H^+ + * + e^- \qquad \text{(I.3)}$$

I.6.2 Cathode Processes

The ORR that occurs at the cathode has a more complicated mechanism and it is well known for its sluggish kinetics. The ORR is the major challenge for PEM fuel cells because the catalyst material must be stable under the extremely corrosive conditions at a fuel cell cathode yet chemically active enough to be able to activate O_2. Due to the difficulties of the ORR, the cathode requires a higher Pt loading, typically more than several times that of the anode .

O_2 adsorbs to the metal surface and the oxygen–oxygen bond breaks to give adsorbed oxygen atoms (O*)

$$½\ O2 + * \rightarrow O* \qquad (I.4)$$

These single oxygen atoms are then protonated by the incoming flow of H^+ across the PEM and reduced by incoming flow of electrons to give surface bound hydroxyl (OH*)

$$O* + H^+ + e^- \rightarrow OH* \qquad (I.5)$$

The surface bound OH* is then further reduced and protonated to give water which then leaves the metal surface,

$$OH* + H^+ + e^- \rightarrow H_2O + * \qquad (I.6)$$

The alternative pathway is an associative mechanism where the O=O bond does not break upon O_2 adsorption onto the metal surface

$$O2 + * \rightarrow O2* \qquad (I.7)$$

$$O2* + H^+ + e^- \rightarrow HO_2* \qquad (I.8)$$

This alternative ‘two electron’ route is observed to produce H_2O_2. The details of the mechanism are unclear, but the reaction may proceed as follows

$$HO_2* + H^+ + e^- \rightarrow H_2O_2* \qquad (I.9)$$

The H_2O_2 may react further:

$$H_2O_2* \rightarrow H_2O_2 + * \qquad (I.10)$$

I.7 Fuel Cell voltage

PEMFCs thermodynamic voltage can be expressed as the following [15]

$$E = 1.229 - 8.5 \times 10^{-4} \times (T - 298.5) + 4.3085 \times 10^{-5} \times T\ [\ln(P_{H2}) + 0.5 \ln(P_{O2})] \qquad (I.11)$$

However, in practice the cell potential is significantly lower than the theoretical potential because there are some losses even when no external load is connected. Moreover, when a load is connected to the fuel cell, the voltage in the terminals decreases still more due to a number of factors, including polarization losses and interconnection losses between cells

I.8 Applications fuel cells

I.8.1 Applications automotive

For automotive traction, only PEMFCs are considered. Their relatively low operating temperature (80 ° C) ensures a greater flexibility of operation. The temperature rise of the battery is easier and faster for "low temperature" batteries than for "high temperature" batteries requiring a large preheating system. A quick start << cold >> is then possible. At the environmental level, noise is low because the applications envisaged do not have moving parts. Only the various auxiliaries of the system can be a source of noise. It should also be noted that the reaction products of the batteries are non-polluting and consequently the harmful gas emissions of the battery alone are zero.

I.8.2 Applications portables

The market for portable electronic devices (telephones, computers, camcorders, electronic diaries, etc.), which is constantly growing, can also be conquered by fuel cells. These devices, with a power range between 0 and 10 W, currently suffer from their low autonomy. On the other hand, with a fuel cell, the autonomy depends only on the size of the fuel tank (hydrogen or methanol). The high modularity of the batteries makes it possible to create small power cells with only a few small cells [16,17].

I.8.3 Applications stationary

Among the stationary applications, it is necessary to distinguish the centralized production of electricity for the industry and the decentralized production, with in particular the stationary applications of weak powers and the cogeneration of medium powers for the residential or for the posts of relief . With regard to centralized electricity generation, some studies envisage replacing polluting power stations with fuel cell systems. However, current installations rarely exceed the power of 1 MW. For these important applications, cogeneration, which allows a recovery of the heat produced, is often used to improve the overall electrical efficiency of the installation.

I.9 Fuel cells efficiency

The efficiency of any energy conversion device is defined as the ratio between the useful energy output and the energy input. in a real system it is necessary to incorporate some auxiliary systems which consume a fraction of the generated power. As a result, the efficiency of the fuel cell system (η_{fc}) [12]

$$\eta_{fc} = \eta_{HHV} \frac{P_{fc} - P_{aux}}{P_{fc}} = \eta_{HHV} \frac{P_{net}}{P_{fc}} \qquad (I.12)$$

Where:
$$\eta_{HHV} = \frac{P_{fc}}{P_{H_2}} = \frac{\frac{V_{fc} I_{fc}}{-\Delta H_{fc} I_{fc}}}{2F_{ar}} = \frac{V_{fc}}{1.482} \qquad (I.13)$$

Where 2 is the number of electrons per molecule of H_2 , F_{ar} is the Faraday number, V_{fc} is the generated voltage and I_{fc} is the fuel cell current

I.10 Advantages & disadvantages

I.10.1 Advantages

•PEM Fuel cells offer very high efficiency possibilities;

•the low operation temperature (below 80◦C)

•There are many sources of fuel and means to feed it;

•They produce no pollutant;

•The cost of the materials is smaller than for the high temperature fuel cells (except the catalyst)

•They require very little maintenance because they have no moving parts;

•They do not need to be recharged and they provide power instantly when fueled

I.10.2 disadvantages

•These fuel cells are relatively expensive because their manufacture requires materials with specific properties.

•It is difficult to find economical replacement materials;

•Fuel reforming can be expensive, difficult and requires energy to operate;

• If fuel other than hydrogen is supplied to the fuel cell, the efficiency decreases with time as the catalyst degrades and the electrolyte becomes oxidized.

I.11 Conclusion

This chapter presents the main concepts about PEM fuel cell systems, showing the structure of these systems. PEM fuel cell have undeniable advantages, system performance, good dynamics and low operating temperature. Regardless of the problem of availability and supply of hydrogen, many points remain to be addressed (cost, mass and volume, service life, thermal management, fluidic management).

CHAPTER II

Lattice Boltzmann Method

II.1 Introduction

Classically, a fluid problem is solved using the derivative equations (EDP) that govern it, like the Navier-Stokes equations. Most traditional resolution methods (finite element method: EF, method of finite differences: DF, finite volume method: VF, ...) in CFD are based on the resolution or of differential or integral forms of the derivative equations partial (EDP). These methods are based on discretization techniques, they EDPs are derived and discretized by finite elements, finite differences or finite volumes usually in regular meshes. The resulting approximate solutions are therefore based on spatial and temporal discretization scales.

New numerical methods, alternatives to classical methods have been developed. These all tend to circumvent the difficulties linked to networking in constructing some or all of the approximation by other approaches than the spatial discretization by elements. Among these methods are the methods called non-mesh methods. These techniques have proved their effectiveness in the treatment of delicate problems to be addressed by conventional methods. Moreover, it is interesting to note that the methodological and / or mathematical concepts used in these very open approaches offer new perspectives for the numerical simulation of the complex phenomena encountered in the flow in porous media[18].

Among the alternative numerical methods, we find the Boltzmann method on a network which is of great interest for the improvement of the study of complex geometries and specifically porous media, this method is completely different from traditional methods as the concept of continuity is abandoned. The main idea of Boltzmann is to bridge the gap between micro and macro approach by not considering each particle behavior alone but behavior of a collection of particles as a unit, this approach is called mesoscopic scale, Figure.II.1 shows the different approach used in simulation of different kind of problems

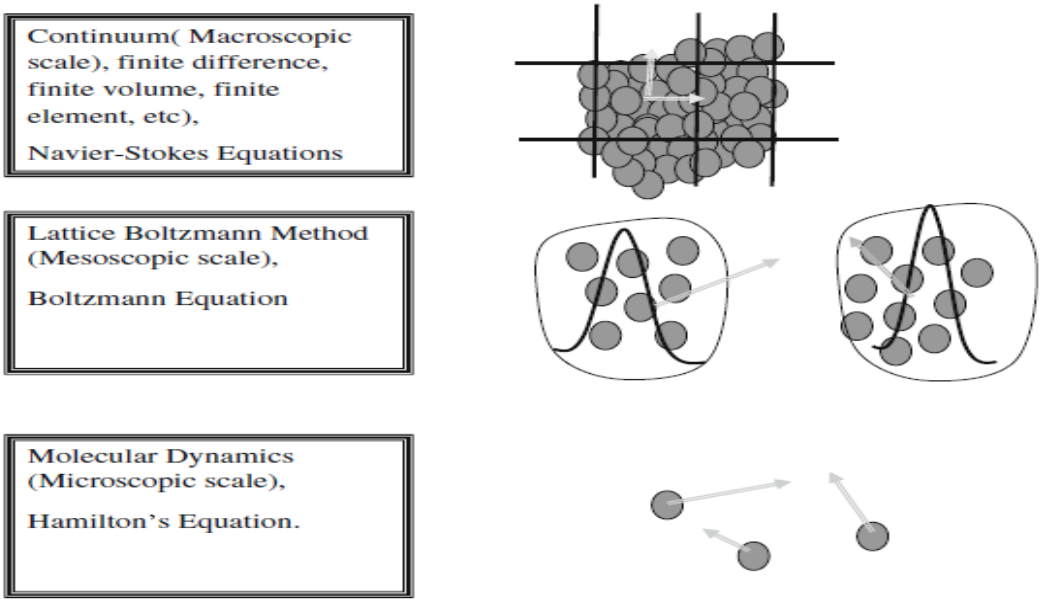

Fig. II.1 Techniques of simulations

II.2 Lattice Boltzmann Method (LBM) :

The dynamics of the lattice Boltzmann method is derived from the equation classic Boltzmann. This equation considers the movement of molecules and describes their behavior statistically following a continuous function in time and space

II.3 Applications of Lattice Boltzmann Method:

The LB method has shown a great ability to simulate systems hydrodynamic [19] , multiphase and multi-component flows[20] , and in porous media [21]. Fig. II.2 shows some areas of application of the LB method.

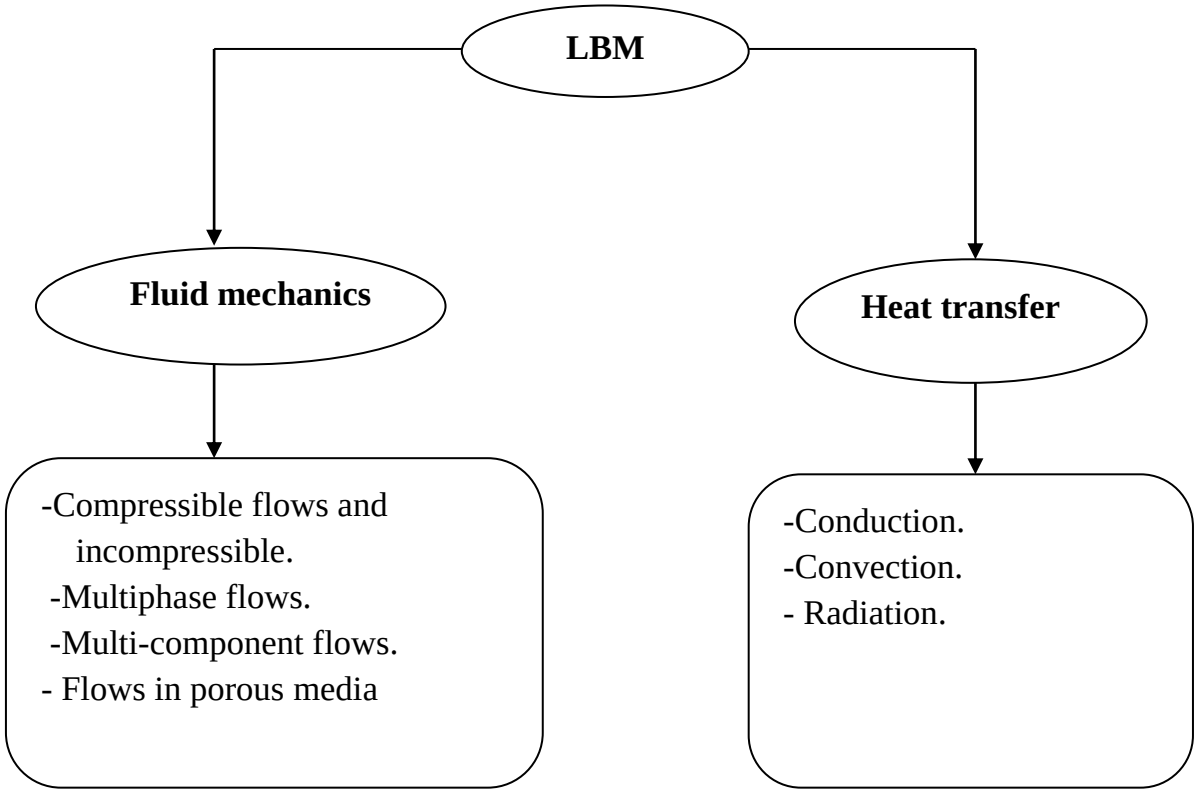

Fig. II.2 Different areas of application LBM

II.4 Boltzmann Equation

A statistical description of a system can be explained by distribution function ***f (x,c,t)***; where ***f (x,c,t)*** is the number of molecules at time t positioned between x and x+dx which have velocities between c and c+ dc. An external force F acting on a gas molecule of unit mass will change the velocity of the molecule from c to c+Fdt and its position from x to x+cdt (Fig.II.3).

The number of molecules ***f (x,c,t)***; before applying the external force is equal to the number of molecules after the disturbance ***f (x+cdt,c+Fdt,t+dt)***; if no collisions take place between the molecules. Hence,

$$f(x+cdt,c+Fdt,t+dt) - f(x,c,t) = 0 \qquad \text{(II.1)}$$

If collisions between particles are accounted then the number of particles in the next step will change and is given by introducing a collision function $\Omega(f)$ which defines as the rate of change of the distribution function

$$f(x+cdt,c+Fdt,t+dt) - f(x,c,t) = \Omega(f) \qquad \text{(II.2)}$$

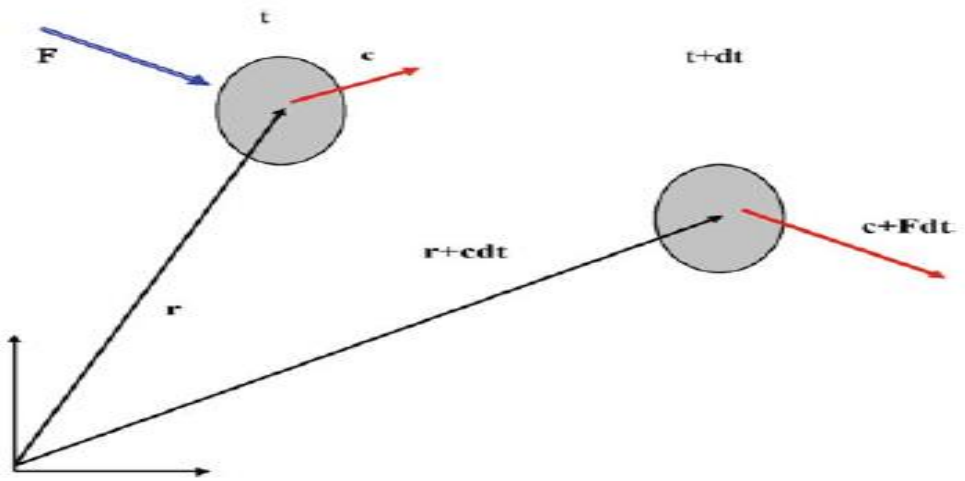

Fig. II.3 particle after and before applying a force [22]

II.4.1 The Boltzmann Transport Equation

Boltzmann's equation describes the evolution of a distribution function of molecule in phase space, which is the superposition of a Euclidean space and a velocity space, given by:

$$\frac{\partial f}{\partial t} + c\frac{\partial f}{\partial x} + \frac{\partial f}{\partial c}\frac{F}{m} = \Omega(f) \qquad \text{(II.3)}$$

For system without an external force, the Boltzmann equation can be written as

$$\frac{\partial f}{\partial t} + c\frac{\partial f}{\partial x} = \Omega(f) \qquad \text{(II.4)}$$

In the Boltzmann BGK model, the term collision replaced by

$$\Omega(f) = \frac{1}{\tau}(f^{eq} - f) \qquad \text{(II.5)}$$

After introducing BGK approximation, the Boltzmann equation (Eq. II.4) can be approximated as,

$$\frac{\partial f}{\partial t} + c\frac{\partial f}{\partial x} = \frac{1}{\tau}(f^{eq} - f) \qquad \text{(II.6)}$$

In Lattice Boltzmann method, the above equation is discretized and assumed it is valid along specific directions, linkages. Hence, the discrete Boltzmann equation can be written along a specified direction as

$$\frac{\partial f_i}{\partial t} + c_i \frac{\partial f_i}{\partial x} = \frac{1}{\tau}(f_i^{eq} - f_i) \qquad \text{(II.7)}$$

One of the major difficulties in dealing with the Boltzmann equation is the complicated nature of the collision term. Therefore, as mentioned previously, an important simplification of collision term was proposed by Bhatnagar, Gross and Krook in 1954 and is known as the BGK approximation. The Boltzmann-BGK equation then takes the form [23]:

$$f_i(x + c_i \delta t, t + \delta t) - f_i(x, t) = \frac{(f_i^{eq}(\rho, \mathrm{u}) - f_i(x, \mathrm{t}))}{\tau_f} \qquad \text{(II.8)}$$

The local equilibrium distribution function with a relaxation time determine the type of problem needed to be solved.

The Boltzmann equation (Eq. II.8) is often described by two different actions taking part at each lattice point (site); namely streaming (propagation) and collision. Streaming describes the movement of the particles of each species and the collision describes the interactions between the particles of the same or different species

Collision step:

$$f_i^*(x, t) = f_i(x, t) \frac{1}{\tau_f}(f_i^{eq}(\rho, u) - f_i(x, \mathrm{t})) \qquad \text{(II.9)}$$

Streaming step:

$$f_i(x + c_i \delta t, t + \delta t) = f_i^*(x, t) \qquad \text{(II.10)}$$

Where $f_i(x, t)$ and $f_i^*(x, t)$ denote the pre-collision and post-collision state of the distribution function, respectively

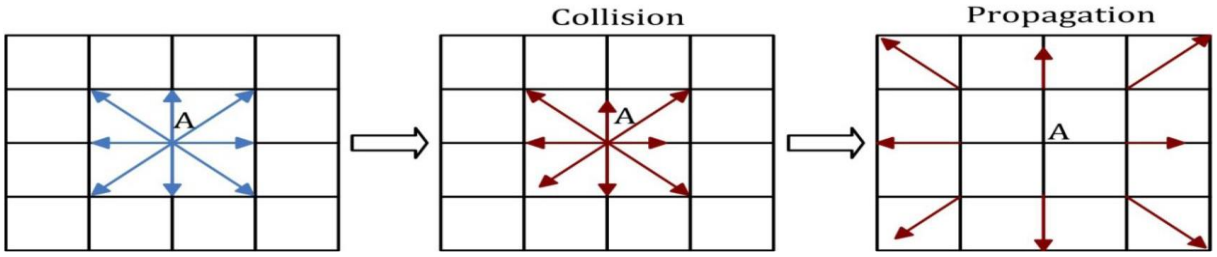

Fig. II.4 Collision and propagation steps [24].

II.4.2 Equilibrium distribution function

The key element in applying LBM for different problems is the equilibrium distribution function, f^{eq}: As we will see in the following this chapter that the procedure of solving diffusion, advection–diffusion, momentum, and energy equations is the same. The difference mainly depends on the equilibrium distribution function. In fact, different physical problems

(such as a wave propagation problem, etc.) can be solved by LBM provided that a proper equilibrium distribution function is used

The general form of the equilibrium distribution function can be written as[22],

$$f_i^{eq} = \phi\omega_i [A + Bc_i u + C(c_i u)^2 + Du^2] \quad \text{(II.11)}$$

where u is the macroscopic flow velocity vector; A, B, C, and D are constants and need to be determined based on the conservation principle (mass, momentum, and energy). ϕ stands for scalar parameter, such as density *(ρ)*, temperature (thermal energy density), or species concentration

II.5 Lattice arrangements

The common terminology used in LBM is to refer to the dimension of the problem and the number of speed is using D_nQ_m, where n represent the dimension of the problem (1 for 1-D, 2 for 2-D and 3 for 3-D) and m refers to the speed model, number of linkages

II.5.1 One-Dimensional

Fig.II.5 illustrates the lattice used for the description of the model D_1Q_3 and D_1Q_2

D_1Q_3

The discrete velocity set and weighting factor

$$\{c_0 = (0,0)c, c_1 = (1,0)c, c_2 = (0,-1)c\} \quad \text{(II.12)}$$

$$\left\{\omega_0 = \frac{2}{3}, \omega_1 = \omega_2 = \frac{1}{6}\right\} \quad \text{(II.13)}$$

D_1Q_2

We speak of the model D_1Q_2 when the particle (0) at rest is not considered. discrete velocity set and weighting factor

$$\{c_1 = (1,0)c, c_2 = (0,-1)c\} \quad \text{(II.14)}$$

$$\left(\omega_1 = \omega_2 = \frac{1}{2}\right) \quad \text{(II.15)}$$

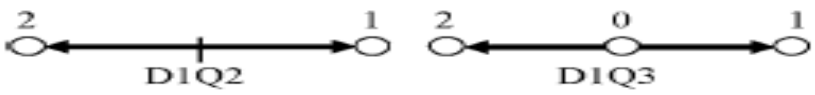

Fig.II.5 : Lattice arrangements for 1-D problems[22]

II.5.2 Two-Dimensional

The discrete velocity set and weighting factor

D_2Q_9

Fig.II.6 shows this model

$$\left.\begin{aligned} &c_0=(0,0)c, c_1=(1,0)c, c_2=(0,1)c, c_3=(-1,0)c, c_4=(0,-1)c, \\ &c_5=(1,1)c, c_6=(-1,1)c, c_7=(-1,-1)c, c_8=(1,-1)c \end{aligned}\right\} \quad (II.16)$$

$$\omega_i=\begin{cases} 4/9 & i=0 \\ 1/9 & i=1 to 4 \\ 1/36 & i=5 to 8 \end{cases} \quad (II.17)$$

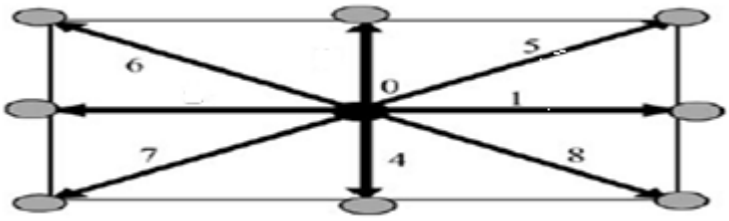

Fig. II.6 Lattice model D_2Q_9[22]

D_2Q_5

Fig.II.7 shows this model

$$\{c_0=(0,0)c, c_1=(1,0)c, c_2=(0,1)c, c_3=(-1,0)c, c_4=(0,-1)c,\} \quad (II.18)$$

$$\omega_i=\begin{cases} 2/6 & i=0 \\ 1/6 & i=1 to 4 \end{cases} \quad (II.19)$$

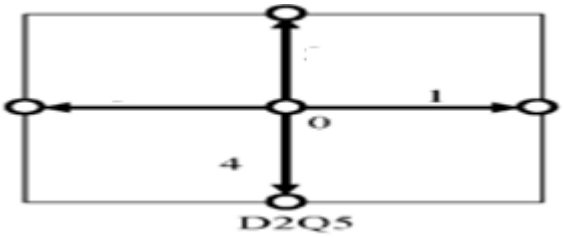

Fig. II.7 Lattice model D_2Q_5

D_2Q_4

Fig.II.8 shows this model

$$\{c_1 = (1,0)c, c_2 = (0,1)c, c_3 = (-1,0)c, c_4 = (0,-1)c,\} \qquad (II.20)$$

$$\{\omega_1 = \omega_2 = \omega_3 = \omega_4 = 1/4\ \} \qquad (II.21)$$

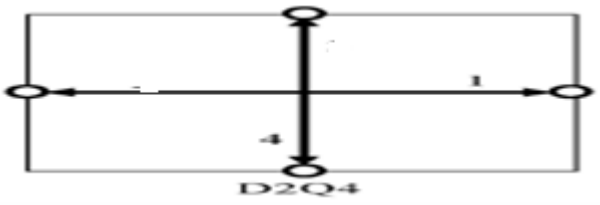

Fig. II.8 Lattice model D_2Q_4

II.5.3 Three-Dimensional

In general two models are used in simulation of three dimensional problems,D_3Q_{15} and D_3Q_{19} The discrete velocity set and weighting factor

D_3Q_{19}

Fig.II.9 shows this model

$$c_i \begin{cases} (0,0,0)\,c & i = 0 \\ (\pm 1,0,0)\,c, (0,\pm 1,0)\,c, (0,0,\pm 1)\,c & i = 1 to 6 \\ (\pm 1,\pm 1,0)\,c, (\pm 1,0,\pm 1)\,c, (0,\pm 1,\pm 1)\,c & i = 7 to 18 \end{cases} \qquad (II.22)$$

$$\omega_i = \begin{cases} 1/3 & i = 0 \\ 1/18 & i = 1 to 6 \\ 1/36 & i = 7 to 18 \end{cases} \qquad (II.23)$$

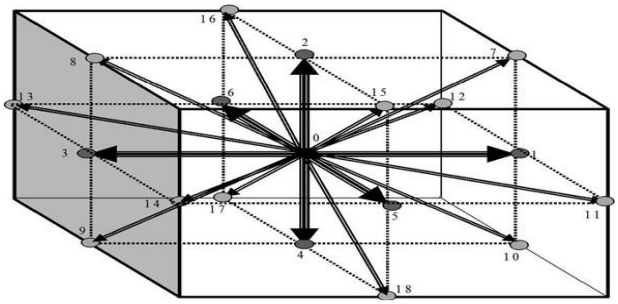

Fig. II.9 Lattice arrangements for 3-D problems, D_3Q_{19}

D_3Q_{15}

Fig.II.10 shows this model

$$c_i \begin{cases} (0,0,0)\,c & i=0 \\ (\pm 1,0,0)\,c,(0,\pm 1,0)\,c,(0,0,\pm 1)\,c & i=1 to 6 \\ (\pm 1,\pm 1,\pm 1) & i=7 to 14 \end{cases} \qquad (II.24)$$

$$\omega_i = \begin{cases} 16/72 & i=0 \\ 8/72 & i=1 to 6 \\ 1/72 & i=7 to 14 \end{cases} \qquad (II.25)$$

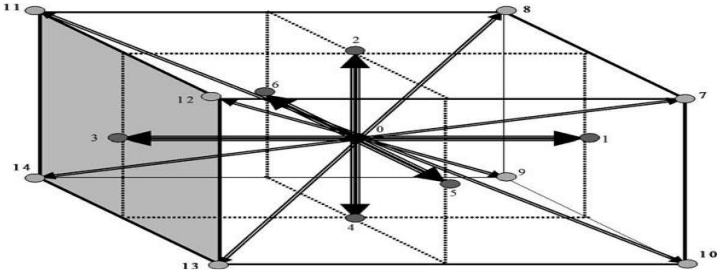

Fig. II.10 Lattice arrangements for 3-D problems, D_3Q_{15}

The equilibrium distributions for all of the D2Q9, D3Q15, D3Q19 and D3Q27 models can be expressed in the following form in which the Navier-Stokes equations can be recovered

$$f_i^{eq}(\rho,u) = \rho\omega_i\left[1+\frac{c_i.u}{c_s^2}+\frac{1}{2}\frac{(c_i.u)^2}{c_s^4}-\frac{1}{2}\frac{u^2}{c_s^2}\right] \qquad (II.26)$$

The macroscopic proprieties such as the local mass density ρ ,the local momentum density ρu can be evaluated as:

$$\rho = \sum_{i=0}^{n} f_i \qquad (II.27)$$

$$\rho u = \sum_{i=0}^{n} f_i c_i \qquad (II.28)$$

The pressure for both models can be calculated as follow:

$$P = c_s^2 \rho \qquad (II.30)$$

Where $c_s = \frac{c}{\sqrt{3}}$ is the sound speed for all these models D_1Q_3, D_2Q_5, D_2Q_9, and D_3Q_{15}[20]

The fluid kinematic viscosity

$$\upsilon = \frac{\delta x^{2}}{3\delta t}(\tau_f - 0.5) \qquad (II.31)$$

II.6 Porous media modeling by LB Method

When applying the LBM to model fluid flows and transport problems in porous media, these are generally two approaches, i.e. the pore scale approach and the representative element volume (REV) scale approach[25] . In the first approach, the standard Lattice Boltzmann equation (LBE) is directly applied to the free fluid in the pores, and the interaction between fluid and the solid matrix is handled by the bounce-back rule. The LBM at the pore scale is the most direct way to modeling fluid flows in particular and transport problems with complex pore geometry. Therefore, this method is effective to study the macroscopic relations and the microscopic mechanism of flow and transport processes through porous media. the LBM at the pore scale has been extensively adopted for investigating transport problems in porous media[26] . However, it needs detailed geometric information of porous matrix, and thus the size of computation domain cannot be too large due to limited computer resources. Another disadvantage of the pore-scale approach is that the volume-averaged velocity cannot be high because the velocity of the free fluid in pores must be small enough due to the low Mach number requirement of LBE [27].

Both limitations of the first approach are overcome by the REV-scale approach where the effects of the porous medium and average transport properties are generally accomplished by including an additional term to the standard lattice Boltzmann equation (LBE). Guo and Zhao developed a LB model to solve incompressible flow in porous media modeling the Navier–Stokes equation at the REV scale, in which the main idea is to include the porosity into the equilibrium distribution functions and add a forcing term to account for the presence of a porous medium[28] . This approach has been proved to be simple and computationally efficient method for modeling and solving transport problems in porous media [29]

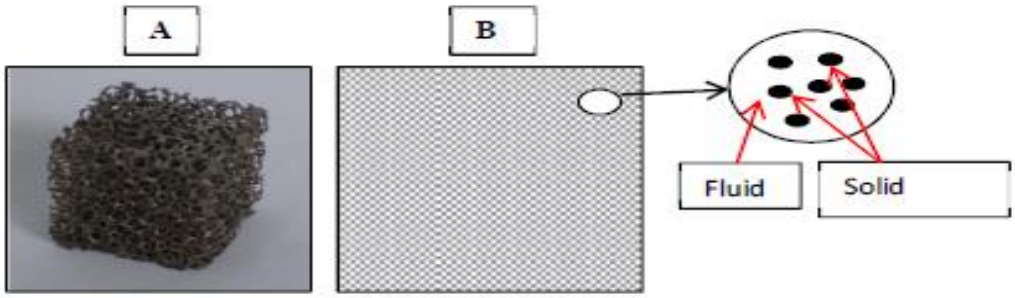

Fig. II.11 porous media modeling: (A) pore scale, (B) representative element volume

II.7 Boundary Conditions

One of the important and crucial issues in LB simulation of flow is accurate modeling of the boundary conditions. Specifying boundary conditions for Navier–Stokes equations is somehow straightforward. This is not the case for LBM, where the inward distribution functions to the integration domain need to be determined at the boundaries. Therefore, we need to determine appropriate equations for calculating those distribution functions at the boundaries for a given boundary condition. In the literature different approaches are suggested and tested. In the following paragraphs, different boundary conditions are explained. The mean idea is not to review different attempts, but to discuss, in our point of view, the simple and more robust methods. Fig.II.12 shows the unknown distribution functions for each side

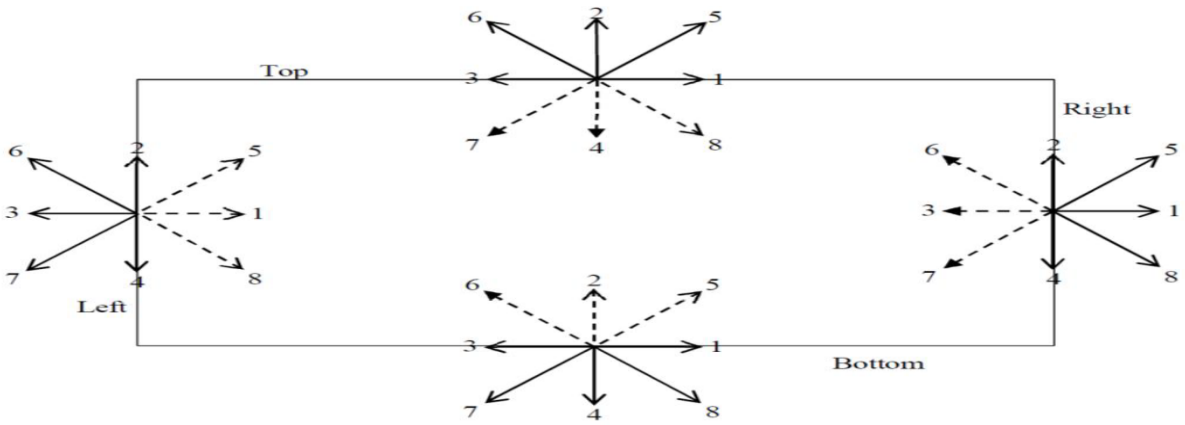

Fig. II.12 Domain boundaries and direction of missing distribution functions

II.7.1 Bounce back

is used to model solid stationary or moving boundary condition, nonslip condition, or flow-over obstacles. The fundamental concept of the bounce back method is mainly implies that an incoming particle towards the solid boundary bounces back into flow domain, Fig.II.13. This boundary condition is relatively easy to implement and is suitable for any kind of geometries. The distribution functions after streaming step can be simply decided as:

$$f_i(x,t) = f_{opp(i)}(x,t)$$

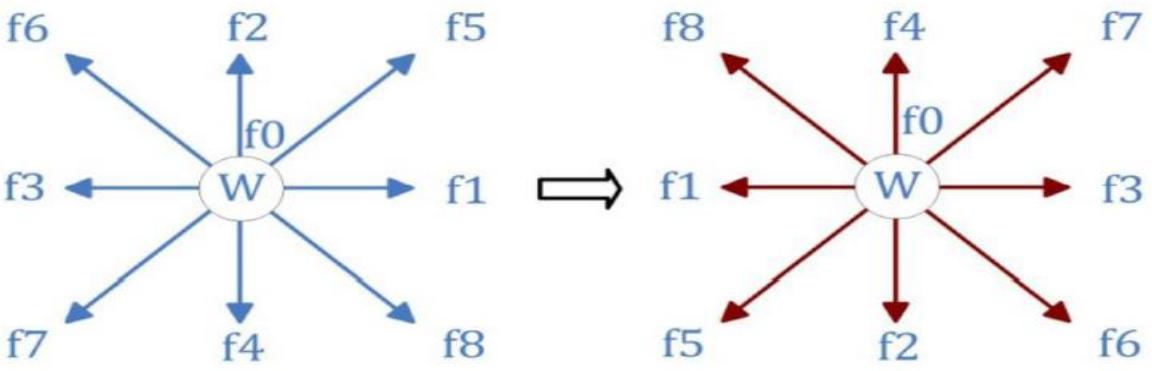

Fig.II.13 Bounce back scheme .The distribution functions are reversed [24]

II.7.2 Boundary condition with known velocity

It is very common in practical applications that we know velocity component at the boundary, for example inlet or outlet condition for a channel flow. Zou and He have proposed a method of specifying velocity on the boundaries for calculate the three unknown distribution functions with equilibrium conditions assumption normal to the boundary. Fig.II.14 shows a domain with east, west, north, and south boundaries[22]

Equation II.27 can be written as

$$\rho = \sum_{i=0}^{8} f_i = f_0 + f_1 + f_2 + f_3 + f_4 + f_5 + f_6 + f_7 + f_8 \qquad (\text{II.32})$$

Equation II.28 can be written for x-component as

$$\rho u = f_1 + f_5 + f_8 - f_6 - f_3 - f_7 \qquad (\text{II.33})$$

and for y-component as

$$\rho v = f_5 + f_2 + f_6 - f_7 - f_4 - f_8 \qquad (\text{II.34})$$

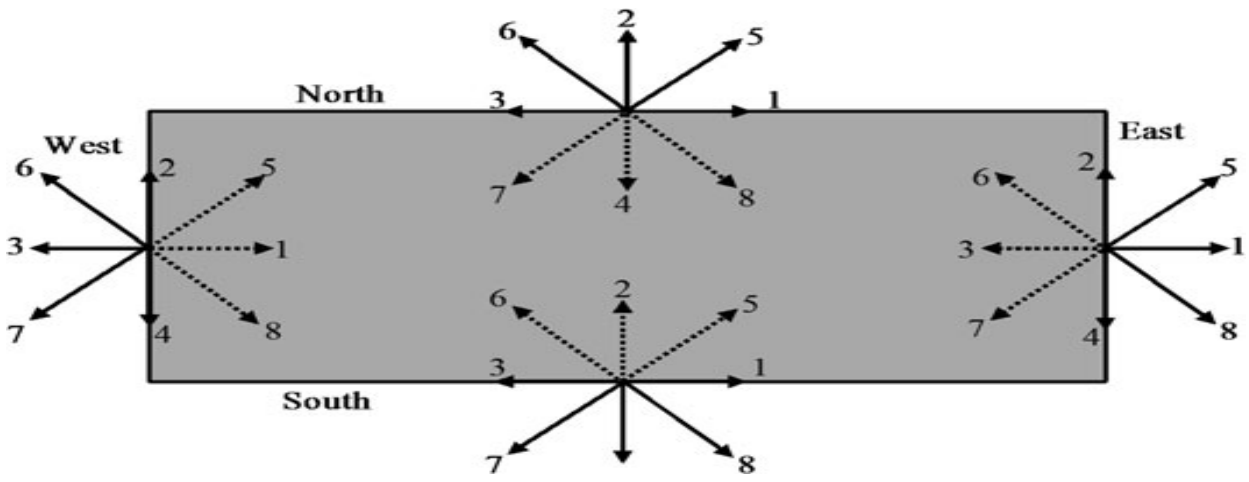

Fig.II.14 Distribution functions at the boundaries of a domain

West Boundary

Then Eq. II.27 can be written as

$$\rho_w = f_0 + f_1 + f_2 + f_3 + f_4 + f_5 + f_6 + f_7 + f_8 \qquad (\text{II.35})$$

Equation II.33 can be written as

$$\rho_w u_w = f_1 + f_5 + f_8 - f_6 - f_3 - f_7 \qquad (\text{II.36})$$

Eq. II.34 can be written as

$$\rho_w v_w = f_5 + f_2 + f_6 - f_7 - f_4 - f_8 \qquad (II.37)$$

The equilibrium condition normal to the boundary, yields

$$f_1 - f_1^{eq} = f_3 - f_3^{eq} \qquad (II.38)$$

Where f^{eq} can be calculated

$$f_1^{eq} = \frac{1}{9}\rho_w \left[1 + 3u_w + \frac{9}{2}u_w^2 - \frac{3}{2}\left(u_w^2 + v_w^2\right)\right] \qquad (II.39)$$

and

$$f_3^{eq} = \frac{1}{9}\rho_w \left[1 - 3u_w + \frac{9}{2}u_w^2 - \frac{3}{2}\left(u_w^2 + v_w^2\right)\right] \qquad (II.40)$$

For the west boundary, the unknown distribution functions are f_1, f_5 *and* f_8 yield the following equations:

$$f_1 = f_3 + \frac{2}{3}\rho_w u_w \qquad (II.41)$$

$$\rho_w = \frac{1}{1-u_w}\left[f_0 + f_2 + f_4 + 2(f_3 + f_6 + f_7)\right] \qquad (II.42)$$

$$f_5 = f_7 - \frac{1}{2}(f_2 - f_4) + \frac{1}{6}\rho_w u_w + \frac{1}{2}\rho_w u_w \qquad (II.43)$$

$$f_8 = f_6 + \frac{1}{2}(f_2 - f_4) + \frac{1}{6}\rho_w u_w - \frac{1}{2}\rho_w u_w \qquad (II.44)$$

East Boundary

$$\rho_E = \frac{1}{1-u_E}\left[f_0 + f_2 + f_4 + 2(f_1 + f_5 + f_8)\right] \qquad (II.45)$$

$$f_3 = f_1 - \frac{2}{3}\rho_E u_E \qquad (II.46)$$

$$f_7 = f_5 + \frac{1}{2}(f_2 - f_4) - \frac{1}{6}\rho_E u_E - \frac{1}{2}\rho_E u_E \qquad (II.47)$$

$$f_6 = f_8 - \frac{1}{2}(f_2 - f_4) - \frac{1}{6}\rho_E u_E + \frac{1}{2}\rho_E u_E \qquad (II.48)$$

North Boundary

$$\rho_N = \frac{1}{1-v_N}[f_0 + f_1 + f_3 + 2(f_2 + f_6 + f_5)] \qquad (II.49)$$

$$f_4 = f_2 - \frac{2}{3}\rho_N u_N \qquad (II.50)$$

$$f_7 = f_5 + \frac{1}{2}(f_1 - f_3) - \frac{1}{6}\rho_N u_N - \frac{1}{2}\rho_N u_N \qquad (II.51)$$

$$f_8 = f_6 + \frac{1}{2}(f_3 - f_2) + \frac{1}{6}\rho_N u_N - \frac{1}{2}\rho_N u_N \qquad (II.52)$$

South Boundary

$$\rho_S = \frac{1}{1-v_S}[f_0 + f_1 + f_3 + 2(f_4 + f_7 + f_8)] \qquad (II.53)$$

$$f_2 = f_4 - \frac{2}{3}\rho_S u_S \qquad (II.54)$$

$$f_5 = f_7 - \frac{1}{2}(f_1 - f_3) + \frac{1}{6}\rho_S u_S + \frac{1}{2}\rho_S u_S \qquad (II.55)$$

$$f_6 = f_8 + \frac{1}{2}(f_1 - f_3) + \frac{1}{6}\rho_S u_S - \frac{1}{2}\rho_S u_S \qquad (II.56)$$

II.7.3 Periodic Boundary Condition

Periodic boundary condition become necessary to apply to isolate a repeating flow conditions. For instance flow over bank of tubes as shown in Fig.II.15 . The flow conditions above the line a and below the line b are the same. Hence, it is sufficient to model the flow between these two lines and use periodic boundary conditions alone these boundaries. The distribution functions that are leaving line a are the same as the distribution functions entering from line b and visa versa.

The distributions functions, f_4; f_7 and f_8 are unknown on the line a and f_2; f_5 and f_6 are unknown on the line b. The periodic boundary is as follows[22]:
along line a:

$$f_{4,a} = f_{4,b}, f_{7,a} = f_{7,b} \text{and} f_{8,a} = f_{8,b}$$

along line b:

$$f_{2,b} = f_{2,a}, f_{5,b} = f_{5,a} \text{and} f_{6,b} = f_{6,a}$$

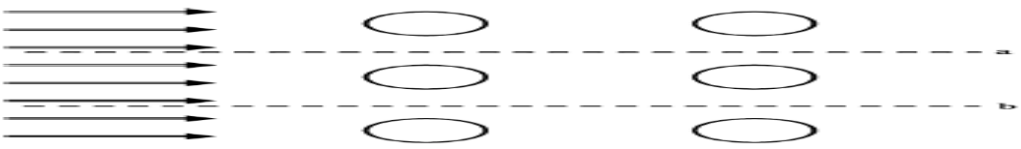

Fig. II.15 Periodic boundary conditions

II.8 Conclusion

Numerical simulation by alternative methods is the subject of numerous research work in the world. When implementing these methods, the fluid and structure domains are no longer represented by a mesh, but by a set of control points representing elementary volumes of matter that are tracked in their movement

For many years, the lattice Boltzmann method (LBM) has been applied successfully to simulate fluid flows and transport phenomena. Unlike conventional methods like CFD, the BR method is based on a mesoscopic approach in which the collective behavior of particles in a system is used to predict macroscopic properties. For this reason, LBM has proved particularly useful in applications relating to the simulation of interface dynamics and complex geometries, for example flows in porous media.

Accurate and efficient boundary conditions development is also important as the development of a precise calculation model, since they will influence the accuracy and stability of the calculation.

CHAPTER III
Numerical simulation and results discussion

III.1 Introduction

The lattice Boltzmann method is a mesoscopic method to describe fluid dynamics and model fluid physics which principle is the resolution of the Boltzmann equation in discretized form at the microscopic scale in order to obtain a solution on a macroscopic scale.

In this method, the fluid is treated as a set of particles moving according to simplified rules in a network composed of solid and fluid nodes. During a time step, the particles propagate towards the neighboring nodes and exchange their momentum during the collision. Every time step the application of external forces to the fluid, can be taken into account if necessary, as well as the different boundary conditions.

III.2 About the code

The fluid flow and heat and mass transfer simulations described in this thesis were computationally performed by the adopted lattice Boltzmann model using the fortran 90 programming language. Intel fortran power station version 4.0 for windows was used for this purpose. Most common features of LBM, collision, propagation, various initial and boundary conditions, calculating macroscopic variables like density, concentration, velocity from the distribution functions were written as different modules and tested. The code algorithms begin with reading the flow parameters like the grid dimensions, fluid proprieties, initial concentration of hydrogen, number of time steps (time of computation), dimensionless relaxation time, data output variables and other specific constants from the input file. Then, the algorithms begin marching in time starting with a collision step where the distributions are collided with their equilibrium values.

Next, the streaming step in which the distribution functions streamed along discrete velocity vectors according to the lattice directions. Different kinds of boundary conditions like Bounce Back, inflow and outflow, constant concentration and periodic boundary conditions are then applied to determine the missing distribution functions from the precedent steps. The remaining step in the code is used to calculate macroscopic variables; these obtained values such as velocity, density and concentration are then used to evaluate the equilibrium distribution function at the beginning of the next time step.

Data utilities were developed to write the output values to file at set intervals. The code has the ability to write the values in *.dat format. These data files are read by software like OriginPro and Tecplot to visualise the results. The following snippet shows the main loop of the code

The algorithm flowchart of the code is given in Fig.III.1

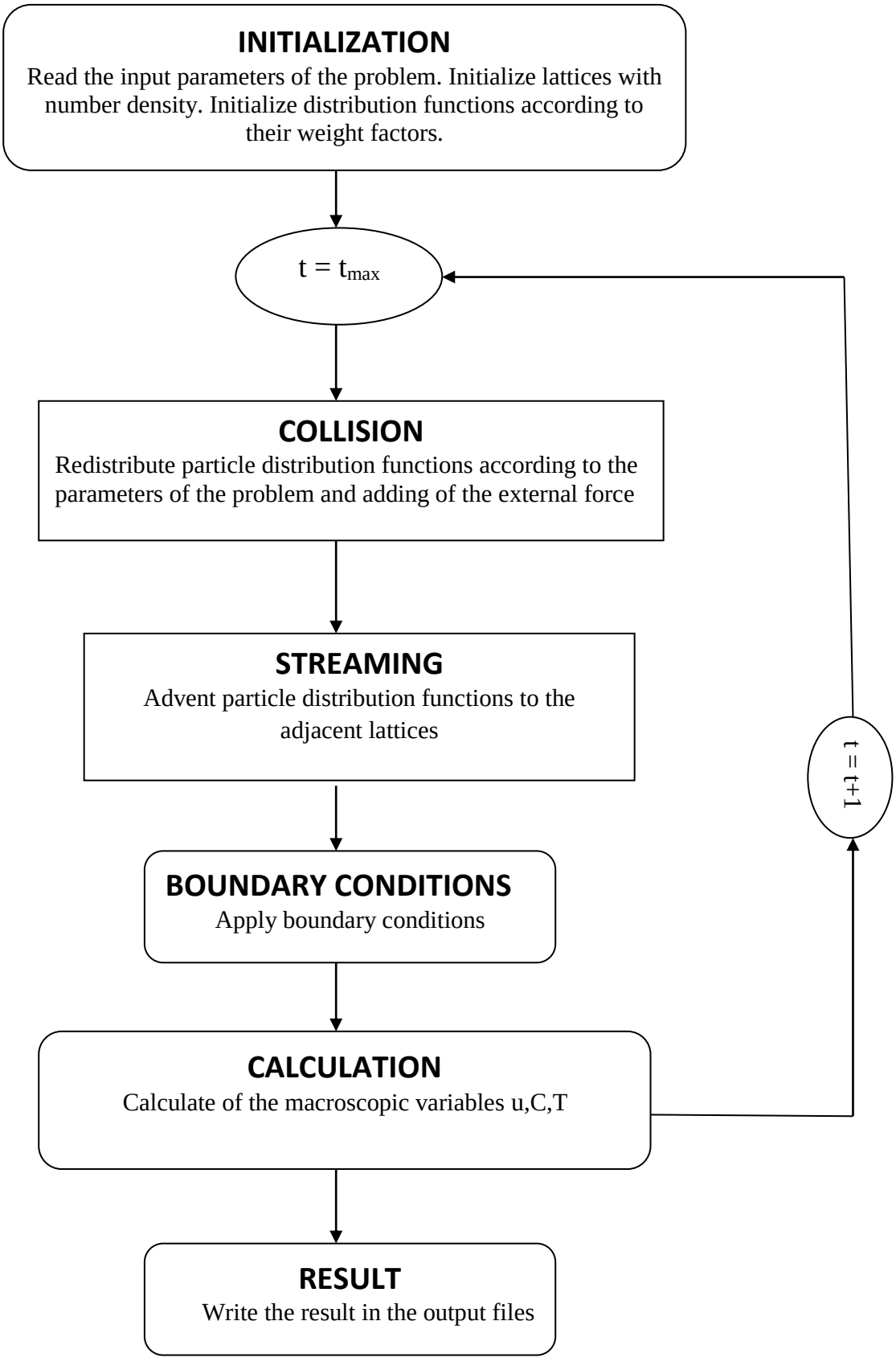

Fig.III.1: Algorithm flowchart of the developed LBM code

III.3 Geometry of the modeled structure

In our study we will focus on gas diffusion layer (GDL) of hydrogen in vertical flow condition**,** This is what the fig III.2 shows

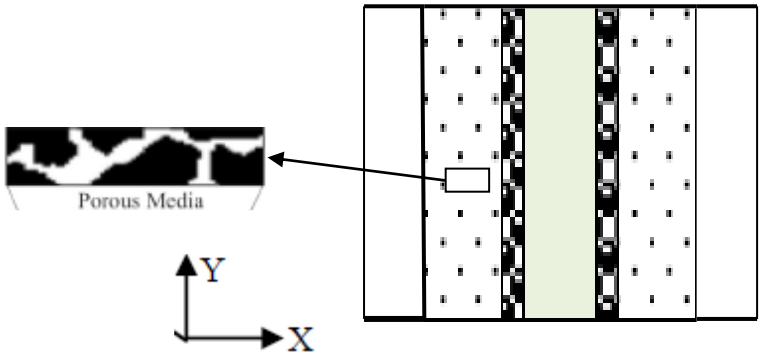

Fig.III.2: 2D schematic of PEMFC. Computational domain shown in rectangle

III.4 Mathematical modeling

III.4.1 Macroscopic equations in porous media

The transport of the different chemical species must be taken into account in the system of equations describing fluid dynamics in channels and porous zones. The model consists of a single system of nonlinear partial differential equations representing the conservation equations of mass, momentum, concentration, and energy. The conservation equations are written [30,31]:

$$\nabla.\mathrm{u} = 0 \qquad \text{(III.1)}$$

$$\partial_t \mathrm{u} + (\mathrm{u}.\nabla)\left(\frac{\mathrm{u}}{\varepsilon}\right) = -\frac{1}{\rho}\nabla(\varepsilon p) + \nu_e \nabla^2 \mathrm{u} + \mathrm{F} \qquad \text{(III.2)}$$

$$\partial_t C + \frac{\mathrm{u}}{\varepsilon}.\nabla C = D_e \nabla^2 C \qquad \text{(III.3)}$$

$$\partial_t \mathrm{T} + \frac{\mathrm{u}}{\sigma}.\nabla \mathrm{T} = \frac{\alpha_e}{\sigma}\nabla^2 \mathrm{T} \qquad \text{(III.4)}$$

Where

$$\mathrm{F} = -\frac{\varepsilon \nu}{k}\mathrm{u} - \frac{1.75}{\sqrt{150\varepsilon k}}|\mathrm{u}|\mathrm{u} + \varepsilon \mathrm{G} \qquad \text{(III.5)}$$

$$\sigma = \left[\varepsilon(\rho c_p)_f + (1-\varepsilon)(\rho c_p)_s\right]/(\rho c_p)_f \qquad \text{(III.6)}$$

$$\alpha_e = \lambda_e / (\rho c_p)_f \qquad \text{(III.7)}$$

$$\lambda_e = \varepsilon\lambda_f + (1-\varepsilon)\lambda_s \qquad \textbf{(III.8)}$$

III.4.2 LB-model in porous media

The Lattice Boltzmann method (LBM) is a recently developed method for simulating fluid flows and modeling physics in fluids. Unlike conventional computational methods which are based on discretisation of macroscopic governing equations, LBM is an approach based on the mesoscopic kinetic equation (Boltzmann equation) for fluids. In the present work a D2Q9 model is used, which has the following set of discrete velocities[32]:

$$\left.\begin{aligned} &c_0 = (0,0)c, c_1 = (1,0)c, c_2 = (0,1)c, c_3 = (-1,0)c, c_4 = (0,-1)c, \\ &c_5 = (1,1)c, c_6 = (-1,1)c, c_7 = (-1,-1)c, c_8 = (1,-1)c \end{aligned}\right\} \qquad \textbf{(III.9)}$$

The dynamics of the flow and the evolution of the velocity field is modeled by the developed lattice Boltzmann equation of a density distribution function by Guo and Zhao [28], given as

$$f_i(x + c_i\delta t, t+\delta t) = f_i(x,t) - \frac{f_i(\mathrm{x,t}) - f_i^{eq}(\rho,\mathrm{u})}{\tau_f} + \delta t\, F_i \qquad \text{(III.10)}$$

τ_f is the dimensionless relaxation time related to the effective viscosity ν_e [33] as

$$\nu_e = (\tau_f - 0.5)\delta x^2 / 3\delta t \qquad \text{(III.11)}$$

$f_i^{eq}(\rho,\mathrm{u})$ is the equilibrium distribution function at location ***x*** and time *t* along the with direction, which is chosen to recover the macroscopic Navier-Stokes equations:

$$f_i^{eq}(\rho,\mathrm{u}) = \rho\omega_i\left[1 + \frac{c_i.\mathrm{u}}{c_s^2} + \frac{1}{2}\frac{(c_i.\mathrm{u})^2}{\varepsilon c_s^4} - \frac{1}{2}\frac{\mathrm{u}^2}{\varepsilon c_s^2}\right] \qquad \textbf{(III.12)}$$

The discrete body force term F_i can be described as [22]

$$F_i = \omega_i\rho\left(1 - \frac{1}{2\tau_f}\right)\left[\frac{e_i.\mathrm{F}}{c_s^2} + \frac{(\mathrm{u.F}:e_i e_i)}{\varepsilon c_s^4} - \frac{\mathrm{u.F}}{\varepsilon c_s^2}\right] \qquad \textbf{(III.13)}$$

To simulate heat transfer within the boundary layer , we have used another distribution function $\mathrm{T_i}(x,t)$:

$$T_i(x + c_i\delta t, t+\delta t) = T_i(x,t) - \frac{T_i(\mathrm{x,t}) - T_i^{eq}(T,\mathrm{u})}{\tau_T} \qquad (i = 0..8) \qquad \text{(III.14)}$$

Where τ_T is the dimensionless relaxation time related to the thermal diffusivity as follow $\alpha_e = \sigma(\tau_T - 0.5)\delta x^2 / 3\delta t$ (III.15)

$T_i^{eq}(\mathrm{T,u})$ is the equilibrium distribution function at location ***x*** and time *t* along the with

direction, which is chosen to recover the macroscopic thermal advection-diffusion equation[31]:

$$T_i^{eq}(T,\mathrm{u}) = T\,\omega_i\left[1+\frac{c_i.\mathrm{u}}{\sigma c_s^2}\right] \qquad \text{(III.16)}$$

In order to simulate the transport of fluid, we have added new distribution function $C_i(x,t)$:

$$C_i(x+c_i\delta t, t+\delta t) = C_i(x,t) - \frac{C_i(\mathrm{x},\mathrm{t}) - C_i^{eq}(C,\mathrm{u})}{\tau_c} \qquad (i=0..8) \qquad \text{(III.17)}$$

Where τ_c is the dimensionless relaxation time related to the effective diffusivity as

$$D_e = (\tau_c - 0.5)\delta x^2 / 3\delta t \qquad \text{(III.18)}$$

$C_i^{eq}(\mathrm{C},\mathrm{u})$ is the equilibrium distribution function at location ***x*** and time *t* along the with direction, which is chosen to recover the macroscopic advection-diffusion equation[31]:

$$C_i^{eq}(\mathrm{C},\mathrm{u}) = C\,\omega_i\left[1+\frac{c_i.\mathrm{u}}{\varepsilon c_s^2}\right] \qquad \text{(III.19)}$$

The macroscopic quantities, fluid density, temperature and concentration, are defined as

$\rho = \sum_{i=0}^{8} f_i, T = \sum_{i=0}^{8} T_i$ and $C = \sum_{i=0}^{8} C_i$ respectively

The fluid velocity ***u*** is calculated using a temporal velocity **v** to consider the effects of porous media [34]:

$$u = \frac{\mathrm{v}}{c_0 + \sqrt{c_0^2 + c_1|\mathrm{v}|}} \qquad \text{(III.20)}$$

$$\mathrm{v} = \sum_{i=0}^{8}(e_i f_i / \rho) + \frac{\delta t}{2}\varepsilon G \qquad \text{(III.21)}$$

Where $c_0 = \frac{1}{2}\left(1+\varepsilon\frac{\delta t}{2}\frac{\upsilon}{k}\right)$ and $c_1 = \varepsilon\frac{\delta t}{2}\frac{1.75}{\sqrt{150\varepsilon^3 k}}$ (III.22)

III.5 Conversion of LB units to physical units

One of the key components for the application of the lattice Boltzmann method to physical problems is the correct conversion from physical world units to lattice units to and vice versa. Because it is not possible to directly input the variables and therefore, scaling has to be applied. Hence, this part of the algorithm procedure needs extra attention.

The fluid viscosity has to be scaled first, we can choose any value less than 0.1 [35]. Having in hand the real values of fluids physical proprieties and the model parameters, we can

define the domain high [m], the fluid kinematic viscosity υ[m^2/s], the strength of external force (gravity) g [m/s^2], the fluid density ρ [kg/m^3], the size of an LBM lattice Δx[m] (resolution dependent). These parameters are used to set a reasonable time step size Δt [s] and limit the mass difference in the simulation Δm[kg] The values of the LBM simulation are dimensionless and they should be converted to the dimensionless values. The following steps show how the physical units (with a subscript ' p ') are transformed to lattice units (with a subscript ' l '): lattice time: $t_l=t_p/\Delta t$ lattice gravity: $g_l=g_p(\Delta t^2/\Delta x)$ lattice diffusion number $D_l=D_p(\Delta t/\Delta x^2)$

III.6 Boundary conditions

Boundary conditions are very important for the stability and accuracy of LBM simulation. The unknown particle distribution functions at the boundary nodes must be calculated through proper boundary conditions. On all solid surfaces, bounce back condition is applied so that the no-slip condition for velocity and insulated condition for concentration and temperature is satisfied.

In the catalyst layer oxidation occurs to the hydrogen.
The transport of H^+ and e^- is not considered. The rate of reaction is dependent on the concentration of the oxygen reaching the surface and the activation over-potential according to the Tafel kinetics is given by:

$$j = j_{0,a}^{ref}\left(\frac{C_{H_2}}{C_{H_2}^{ref}}\right)^{1/2}\exp\left(\frac{\alpha_a F_{ar}\eta}{RT}\right) \qquad \text{(III.23)}$$

The over-potential value depends on the operating voltage as[30]:

$$\eta = V_{op} - U_0 \qquad \text{(III.24)}$$

The reaction causes heat generation due to the irreversible heat of electrochemical reaction and the reversible entropic heat. Joule heating is not considered in the present work. The total heat generated will then be given by[30]:

$$Q = j\left(\eta + \mathrm{T}\frac{\partial \mathrm{U}_0}{\partial \mathrm{T}}\right) \qquad \text{(III.25)}$$

And the temperature dependence of open circuit voltage is given by[30]:

$$\mathrm{U}_0 = 0.0025\mathrm{T} + 0.2329 \qquad \text{(III.26)}$$

III.7 Modeling parameters

Among the most tedious parts of model development is determining the correct parameters for the model, which will eventually determine the accuracy of the results.

Table III.1 Values of Parameters Used for simulation[36]

Parameters	Fluid properties
μ (Kg/m s)	8.411E-6
ρ (Kg /m^3)	0.08189
D (m^2 / s)	1.1028E-4
λ (W/m K)	0.1672
c_p (j/ Kg K)	14283
T (K)	353
	Boundary layer formation properties
	gas diffusion layer
ρ (Kg /m^3)	2000
λ (W/m K)	65
c_p (j/ Kg K)	840
porosity	0.4
Permeability (Darcy)	17.6
Thickness (m)	4E-4
Height (m)	1E-3
	Catalytic layer
ρ (Kg /m^3)	387
λ (W/m K)	0.2
c_p (j/ Kg K)	770
porosity	0.4
Permeability (Darcy)	17.6
Thickness (m)	0.6E-4

III.8 Numerical Results and Discussion

In this section we will discuss thermo-fluidic behavior, concentration , velocity of gas hydrogen and the temperature . where we will take period of time to study the velocity, concentration and the temperature (250000 time l.u) under different effects, where x< 40 is thickness of GDL , x > 40 is thickness of catalyst layer and V_{op}= 0.5 V, anodic layer (GDL and catalyst layer)

III.8.1 Effect of Permeability

the following is the distribution velocity and concentration as well as temperature gas of hydrogen obtained by simulation, for different Permeability values(k =1.76,8.8and17.6 Darcy) in thickness of anodic layer

III.8.1.1 Distribution velocity of hydrogen

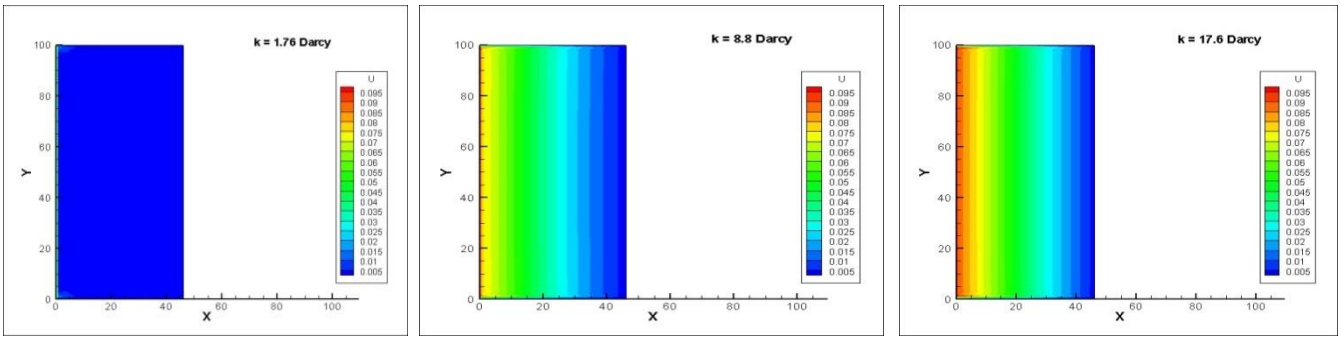

Fig.III.3: Distribution velocity horizontal of hydrogen in anodic layer for different permeability values

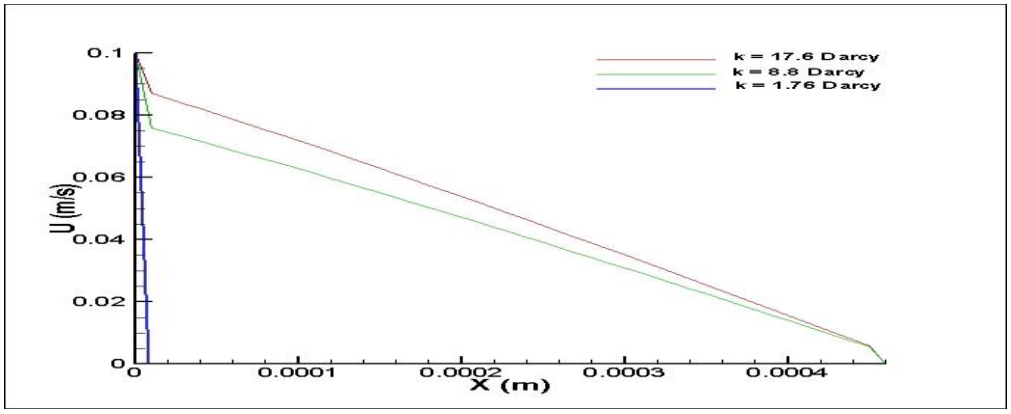

Fig.III.4: Profiles velocity horizontal of hydrogen in anodic layer for different permeability values

Figure (III.3,III.4) shows the distribution velocity of hydrogen in anodic layer.We can see that when the permeability increased the horizontal gradient velocity within GDL thickness increased also; this behavior demonstrated that the improvement of permeability allows and facilitates the fluids flows.

III.8.1.2 Distribution concentration of hydrogen

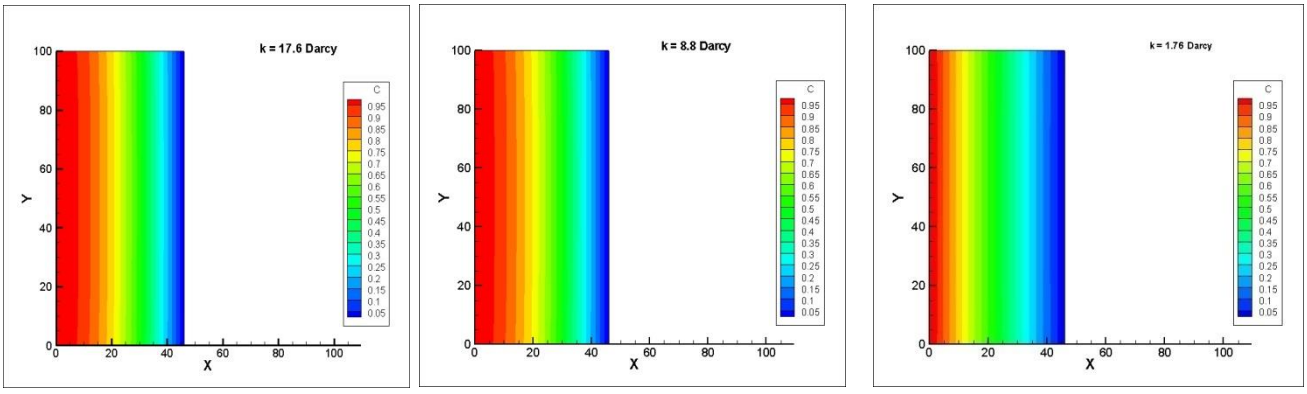

Fig.III.5: Distribution the fraction concentration of hydrogen in anodic layer for different permeability values

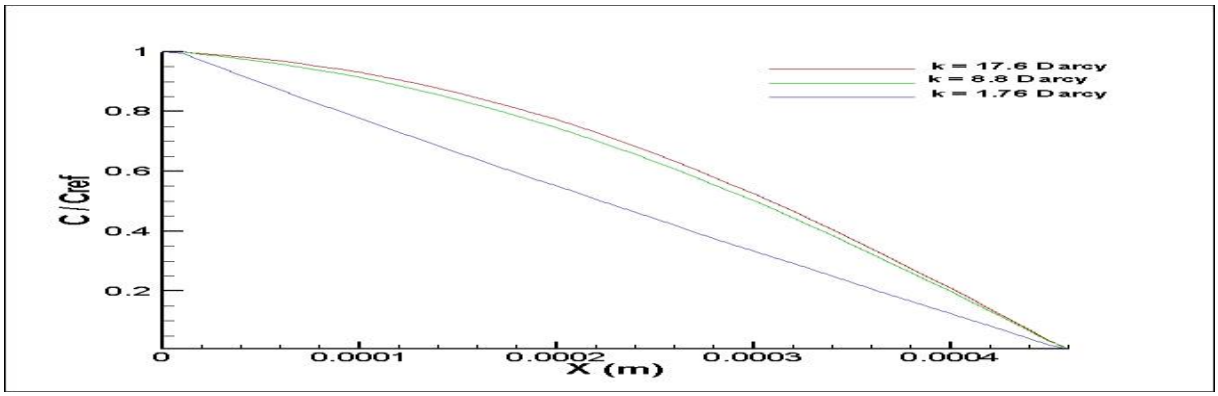

Fig.III.6: Profile the fraction concentration of hydrogen in anodic layer for different permeability values

Figure (III.5, III.6) shows the distribution of the fraction concentration of hydrogen in anodic layer. We can observe the same remarks as the previous results. In other side, we can show a relative concordance between the permeability of 8.8 Darcy and 17.6 Darcy, as consequence a permeability of 8.8 Darcy is sufficient for give as a good distribution of hydrogen in GDL.

III.8.1.3 Distribution temperature of hydrogen

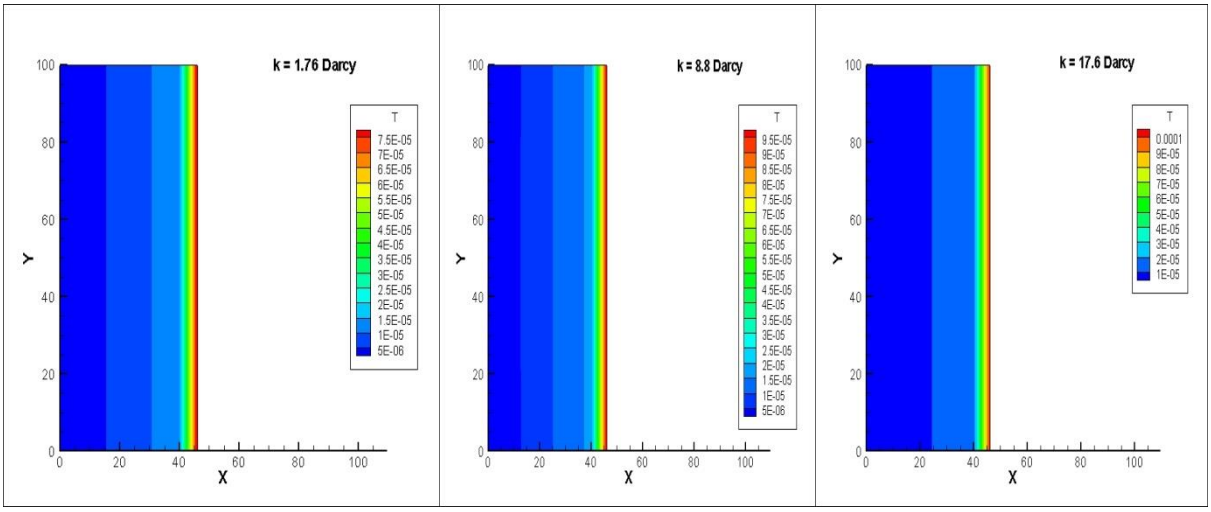

Fig.III.7: Distribution temperature dimensionless of hydrogen in anodic layer for different permeability values

This figure shows that permeability has a positive effect on the dimensionless distribution of temperature of hydrogen. Where increased permeability led to increased dimensionless temperature of hydrogen in GDL . This is due to an increase to hydrogen transfer in catalyst layer resulting increased the hydrogen oxidation ,where we find relative convergence the maximum temperature at the permeability of 8.8 Darcy and 17.6 Darcy.

III.8.2 Effect of porosity

In the following, we will study the influence of porosity on the distribution velocity, concentration and temperature of hydrogen gas in the GDL. Three different values of porosity(ε = 0.4, 0.6 and 0.8) were chosen for this study.

III.8.2.1 Distribution velocity of hydrogen

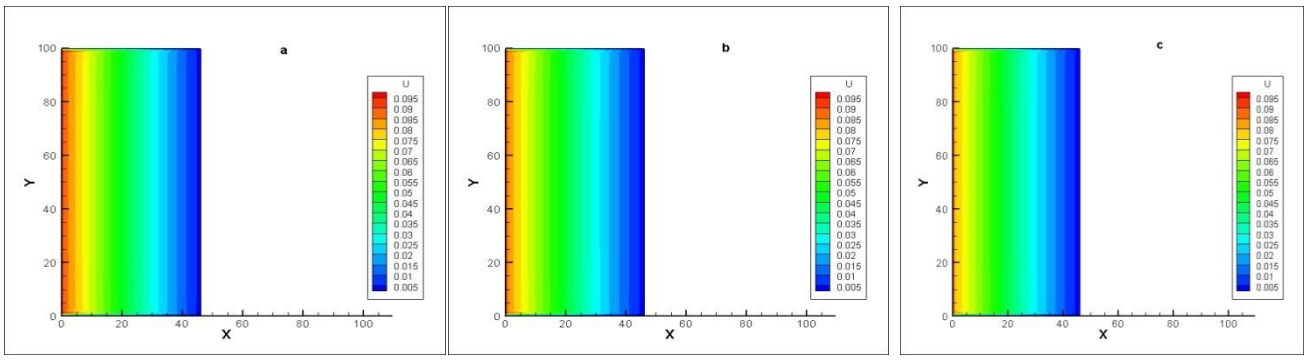

Fig.III.8: Distribution velocity horizontal of hydrogen in anodic layer for different porosity values ε = a)0.4,b)0.6, c)0.8

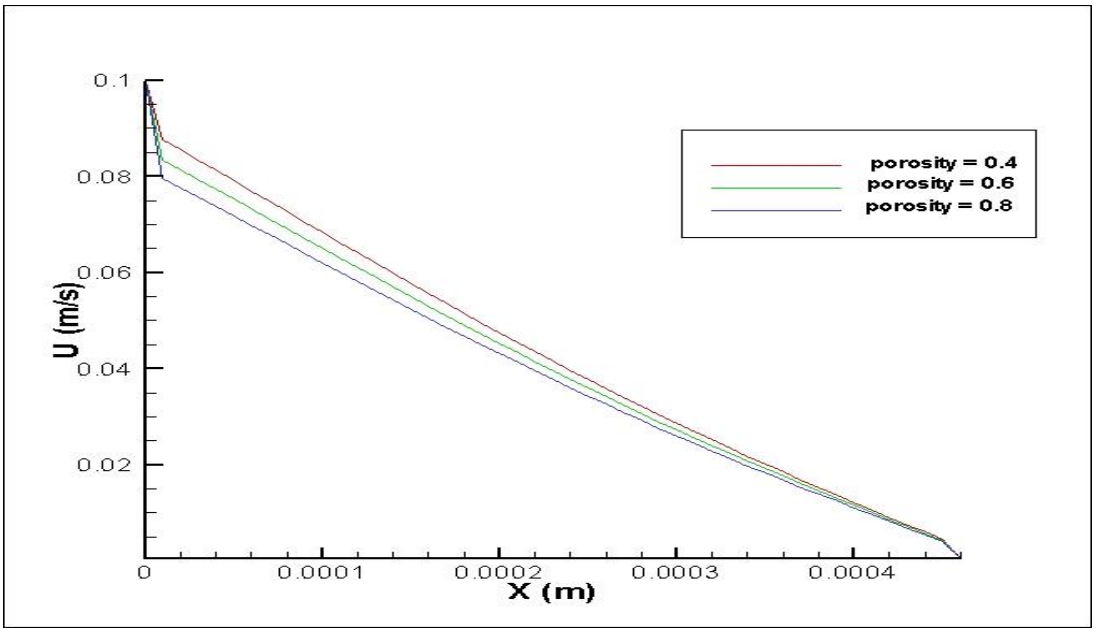

Fig.III.9: Profile velocity horizontal of hydrogen in anodic layer for different porosity values

I noticed from the contours in Fig III.8 that the porosity has a negative effect on the gradient, where we found that the increase in porosity led to a decrease in the gradient velocity horizontal of hydrogen in the GDL and the reason for the increase in the size of the voids and this is confirmed by Fig III.9

III.8.2.2 Distribution concentration of hydrogen

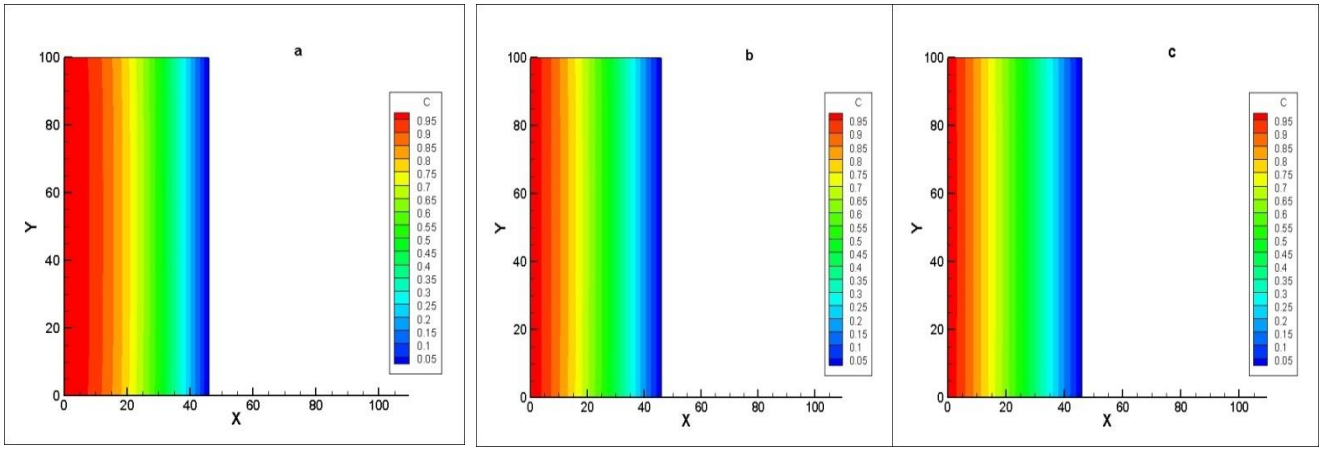

Fig.III.10: Distribution the fraction concentration of hydrogen in anodic layer for different porosity values ε = a)0.4,b)0.6, c)0.8

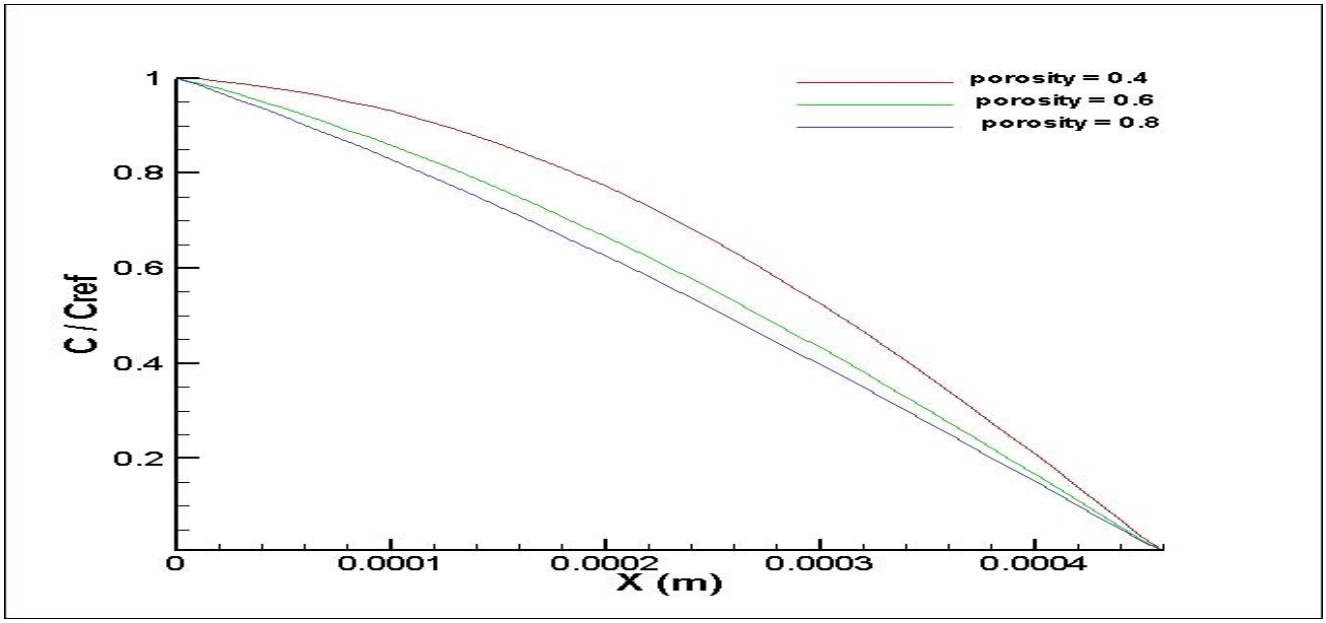

Fig.III.11: Profile the fraction concentration of hydrogen in anodic layer for different porosity values

Fig.III.10 shows the variation in hydrogen concentration distribution as the porosity value in the porous medium changes. It is seen that as the porosity increases, the amount of hydrogen transport into the porous GDL is reduced, as shown in (Fig.III.11). Where we find the porosity value (ε =0.4) is appropriate

III.8.2.3 Distribution temperature of hydrogen

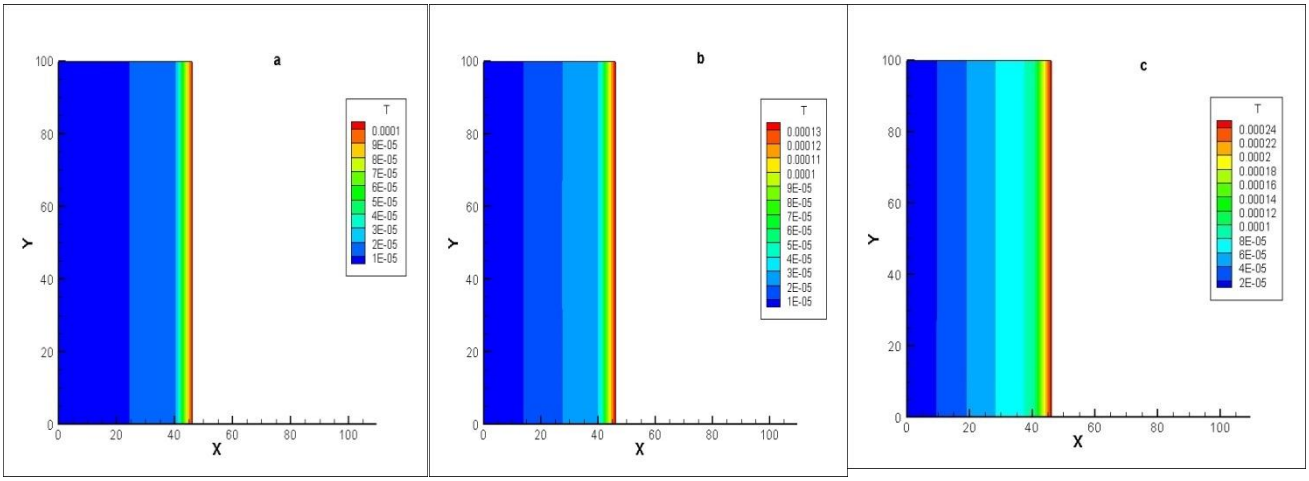

Fig.III.12: Distribution temperature dimensionless of hydrogen in anodic layer for different porosity values ε = a)0.4,b)0.6, c)0.8

Figure (III.12) shows the variation in hydrogen temperature dimensionless distribution as the porosity value in the porous medium changes. It is seen that as the porosity increases, the temperature dimensionless of hydrogen into the porous GDL is increased, where temperature dimensionless has reached a value of 0.00024 in catalyst layer at ε = 0.8

III.8.3 Effect of gas inlet velocity

This section represents the distribution of concentration as well as temperature of hydrogen gas obtained by LB simulation, for different inlet velocity values (u = 0.1,0.05 and 0.01 m/s) in the thickness of anodic layer

III.8.3.1 Distribution concentration of hydrogen

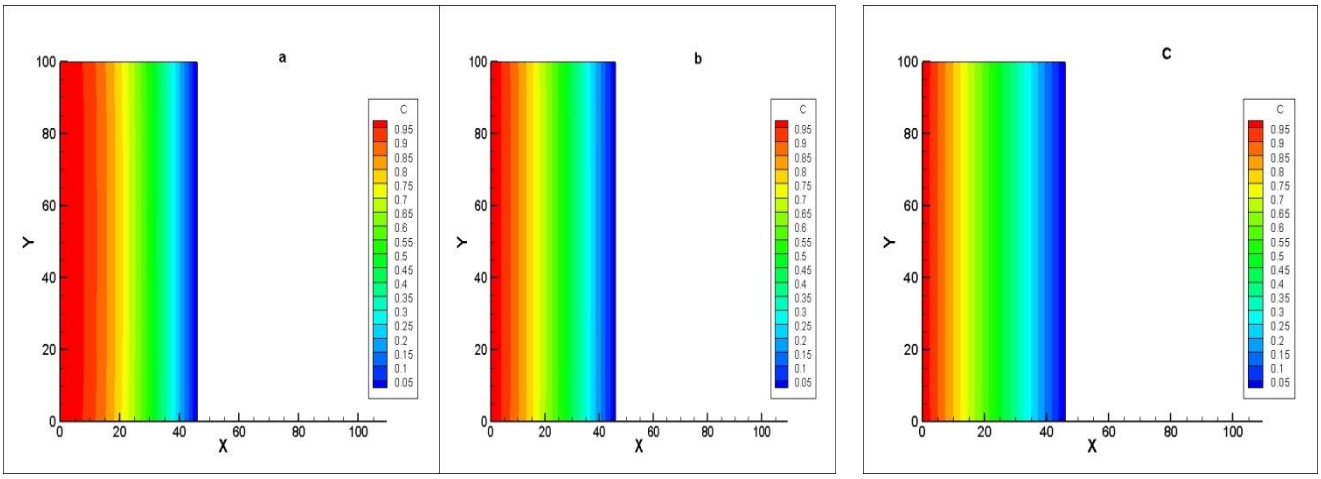

Fig.III.13: Distribution the fraction concentration of hydrogen in anodic layer for different gas inlet velocity values u = a)0.1,b)0.05, c)0.01 m/s

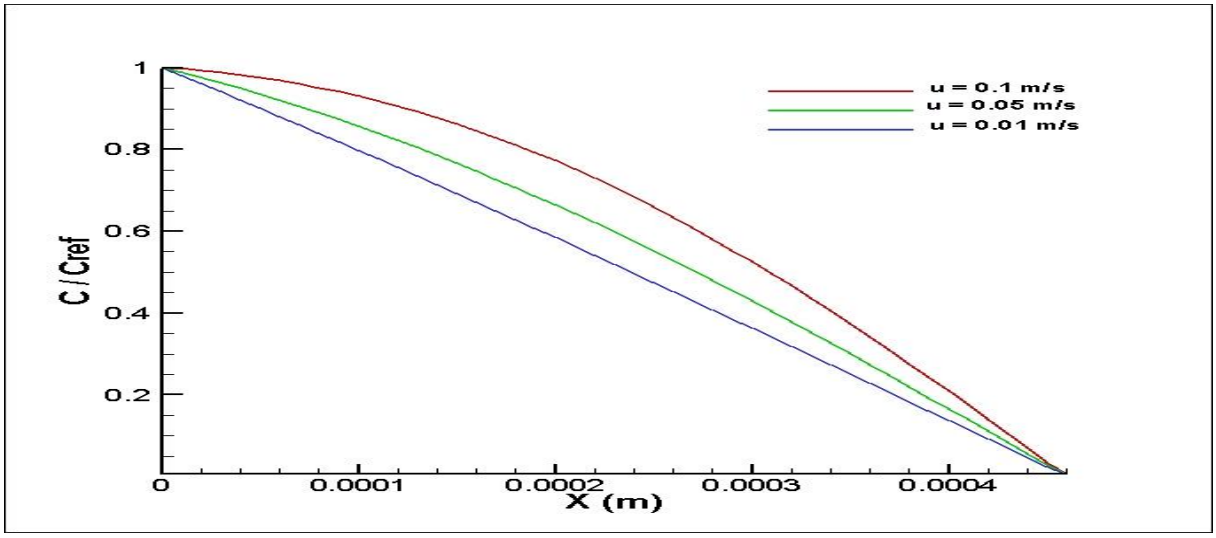

Fig.III.14: Profile the fraction concentration of hydrogen in anodic layer for different gas inlet velocity values

The hydrogen fraction concentration distribution in the computational domain is shown in Fig (III.13,14) for the three inlet velocity. The figure shows that the inlet velocity has a strong influence on the hydrogen transport ,when the inlet velocity increased the gradient concentration within GDL thickness increased Therefore, we use the highest possible velocity while taking endurance

III.8.3.2 Distribution temperature of hydrogen

FigIII.15 shows that the dimensionless temperature increases in the catalyst layer with increasing of inlet velocity, this is due to the reaction rate in this region will also be increased due to reactant concentration.

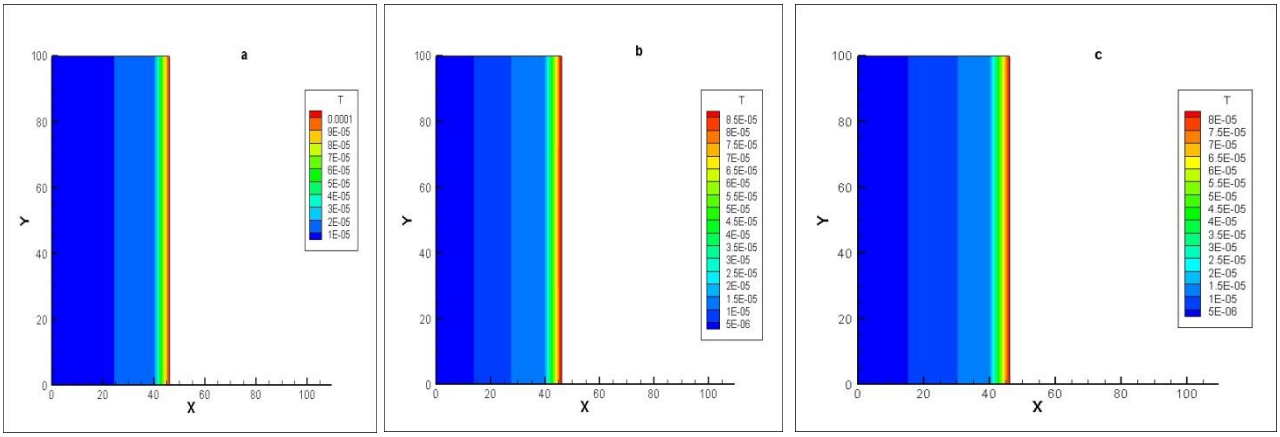

Fig.III.15: Distribution temperature dimensionless of hydrogen in anodic layer for different gas inlet velocity values u = a)0.1,b)0.05, c)0.01 m/s

III.8.4 Effect of height electrode

The effect of electrode height on velocity distribution, concentration and temperature of hydrogen gas will be disused hear for different electrode height values (H,2H and 2.5H).

III.8.4.1 Distribution velocity of hydrogen

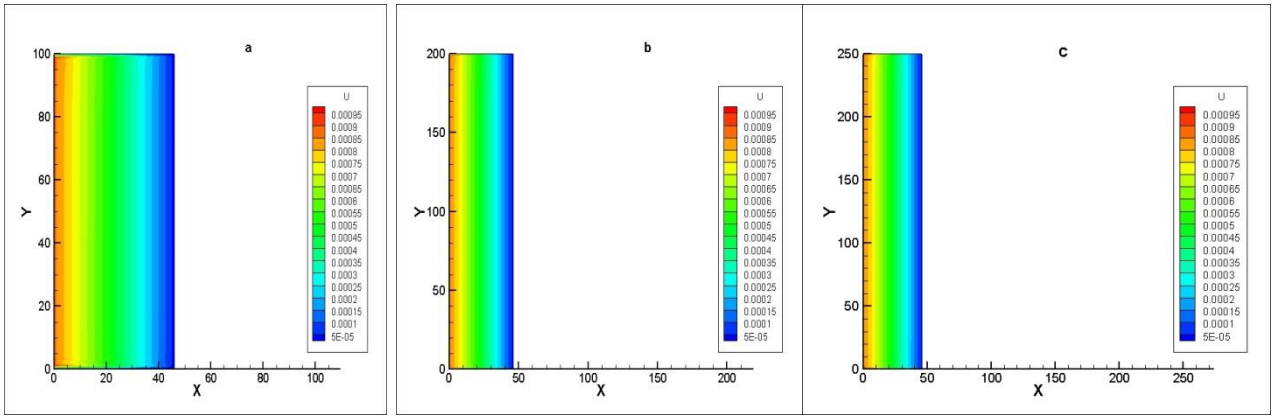

Fig.III.16: Distribution velocity horizontal of hydrogen in anodic layer for different height electrode values a)H , b)2H , c)2.5H

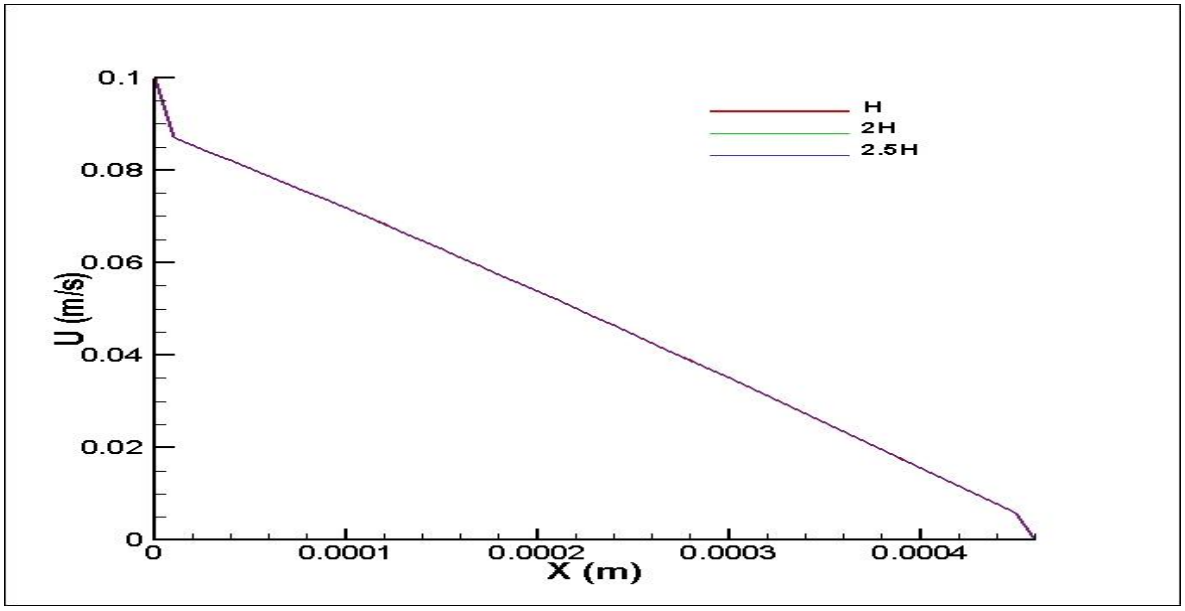

Fig.III.17: Profile velocity horizontal of hydrogen in anodic layer for different height electrode values

The simulation results show that the height change does not affect gradient velocity horizontal of hydrogen in the anode layer (GDL and catalyst layer)and this is shown in Fig.III.16,17 ,where a match appears in the gradient with increased height

III.8.4.2 Distribution concentration of hydrogen

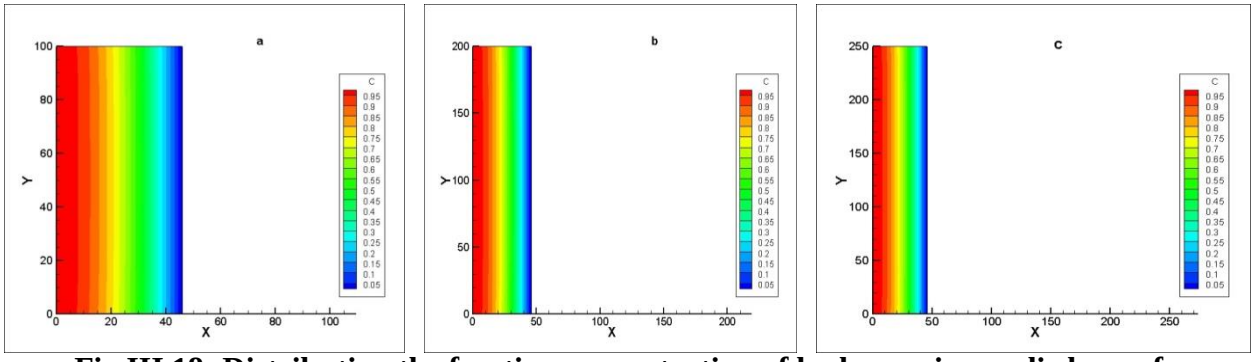

Fig.III.18: Distribution the fraction concentration of hydrogen in anodic layer for different height electrode values a)H , b)2H , c)2.5H

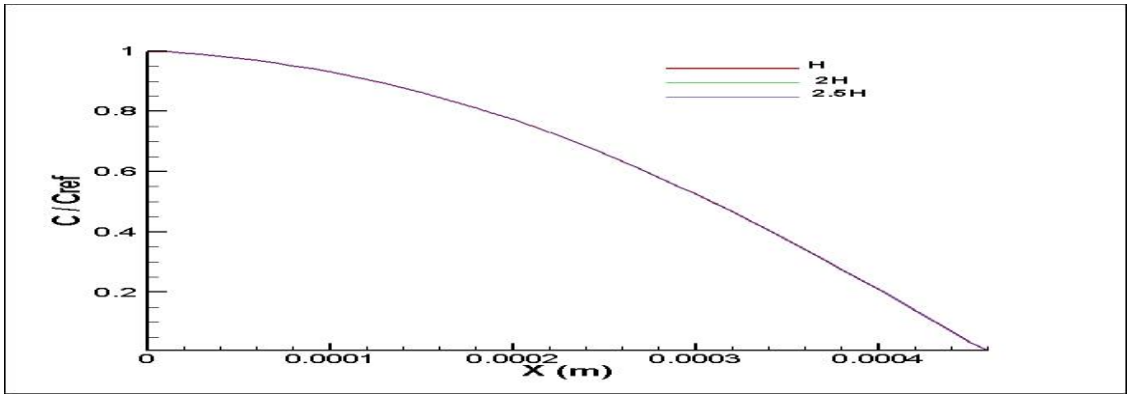

Fig.III.19: Profile the fraction concentration of hydrogen in anodic layer for different height electrode values

As in previous, the simulation results(Fig.III.18,19) show that the height change does not affect gradient the fraction concentration of hydrogen in anode layer

III.8.4.3 Distribution temperature of hydrogen

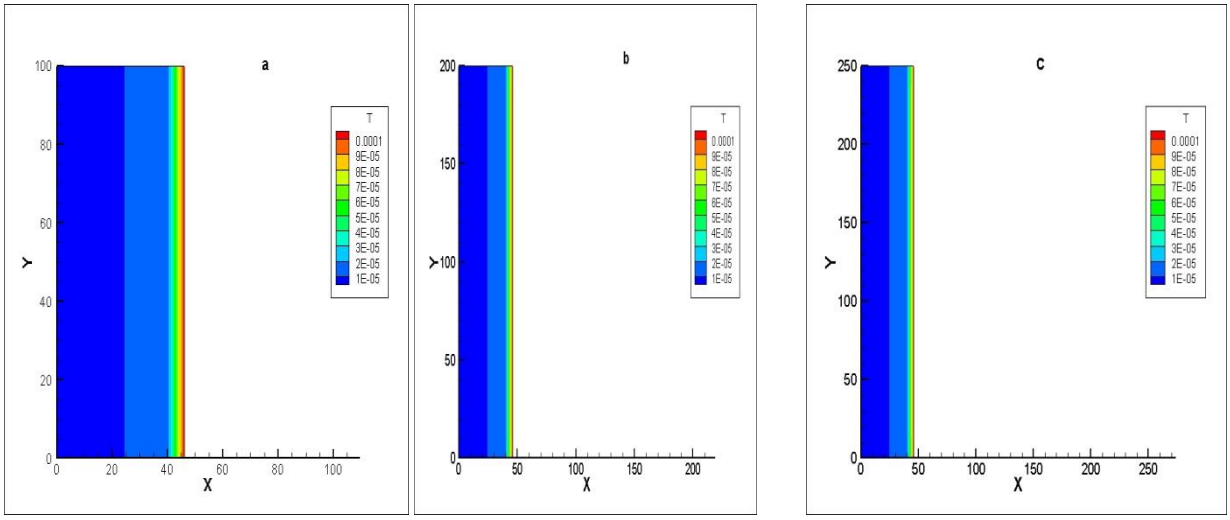

Fig.III.20: Distribution temperature dimensionless of hydrogen in anodic layer for different height electrode values a)H , b)2H , c)2.5H

Figure (III.20) shows the distribution of hydrogen temperature in the anode layer (GDL and catalyst layer) shows along the flow direction of three different height electrode values. It is seen that there is no apparent effect of height on the temperature values in the anode layer

III.9 Conclusion

A parametric study was performed using a LBM (lattice Boltzmann method) model bi-dimensional on the anodic layer. The distribution of velocity, concentration and temperature was introduced inside anodic layer for various parameters. This model used to provide a basic understanding of transport phenomena that occur in the fuel cell. The simulation results show a good match between model and known responses, so that our model can predict the performance of fuel cells under different effects

General conclusion

General conclusion

The main objective of this work is to give a look at the thermo-fluidic behavior of gas flow in Gas Diffusion Layer (GDL). A number of simulation studies were carried out to understand the various transport phenomena using Lattice Boltzmann Method

We can conclude from the first chapter ,how the fuel cell works and the main components and their properties in terms of material and its importance in the physical phenomena that occur in the cell and electrochemical reactions that generate electricity and advantages & disadvantages of PEM fuel cell

In second chapter, the choice of Lattice Boltzmann method was based on several points, it's clear mathematical and physical modeling, it's easy programming, parallelization and high computational efficiency, it's ability to integer complex geometry and implementation of the boundary conditions in this geometry

The simulated results with the adopted LBM model presented in third chapter , the simulation results showed the effectiveness of increasing inlet gas velocity and permeability on gradient velocity , concentration and temperature . On the other hand we found that porosity has a positive effect on temperature gradient and a negative effect on the velocity gradient and concentration. Form the obtained results, we don’t show a clear effect of the height of the electrode on different obtained simulation results under mentioned conditions.

References

[1] P.Thounthong, Conception d'une source hybride utilisant une pile à combustible et des supercondensateurs , *doctorat de l'institut National polytechnique de Lorraine*, 2005.

[2] U.S. department of energy, Hydrogen Fuel Cell Engines and Related Technologies Course Manual, disponible à: http://www.eere.energy.gov/ hydrogen and fuel cells/fuel cells/.

[3] A. Alanazi, E. Ogungbemi, A. Wilberforce, O. Ijaodola, P. Vichare & A. Olabi , hydrogen and fuel cells, international conference on sustainable energy and environmental protection (june 27th – 30th, 2017, bled, slovenia)

[4] Blunier B., Miraoui A., *20 questions sur la pile combustible*, Techip, 2009.

[5] C. J. Andrews et S. A. Weiner, Visions of hydrogen future, *IEEE Power & Energy Magazine*, pp. 26-34, mars-avril, 2004.

[6] J. H. Gurney, Building a case for the hydrogen economy, *IEEE Power & Energy Magazine*, pp. 35-39, mars-avril, 2004.

[7] A. T-Raissi et D. L. Block, Hydrogen: automotive fuel of the future, *IEEE Power & Energy Magazine*, pp. 40-45, novembre-décembre, 2004.

[8] Jiao K, Ni M. Challenges and opportunities in modelling of proton exchange membrane fuel cells (PEMFC). *Int J Energy Res*. 2017;41:1793–1797

[9] Larminie J., Dicks A., *Fuel Cell Systems Explained*, Wiley, 2nd Edition, 2003.

[10] Blunier B., Miraoui A., *Pile à combustible: principes, technologies modélisation et application*, Ellipses-Technosup, Paris, 2007.

[11] Y.Wang, S.Basu, C.Y.Wang, Modeling two-phase flow in PEM fuel cell channels, *Journal of Power Sources*, 179 (2008) 603–617

[12] Barbir F., *PEM Fuel Cells: Theory and Practice*, Academic Press,2005.

[13] Stevens P., Novel-Cattin F., Hammou A., Lamy C., Cassir M., Piles à combustibles, Technical Report, Techniques de l'ingénieur, 2000.

[14] Oliver T. Holton and Joseph W. Stevenson, *The Role of Platinum in Proton Exchange Membrane Fuel Cells*, *Platinum Metals Rev*., 2013, **57**, (4), 259–271

[15] Correa J, Farret F,Canha L, SimoesM (2004)An electrochemical-based fuel-cell model suitable for electrical engineering automation approach. Ind Electron, IEEE Trans on 51(5):1103–1112

[16] C. Roux, D. Marsacq, J. Y. Laurent, C. Nayose, D. Bloch, and J. Arroyo, Application of electrochemical and microelectronic processes to mems fuel cell conception, In France-Deutschland Fuel Cell Conference, Octobre, 2002.

[17] J. P. Meyer and H. L. Maynard, Design considerations for miniaturized pem fuel cells, *Journal of Power Sources*, 109:76-88, 2002.

[18] M .Cherbi, Simulation par la méthode de Boltzmann sur réseau de l´écoulement près des perforations d´un puits d´huile soumis à une opération de fracturation hydraulique, mémoire magister, Universite Kasdi Merbah Ouargla , 2014

[19] R. Benzi, S. Succi, and M. Vergassola, Lattice-Gas Cellular Automata and Lattice Boltzmann Models, Phys. Rep. 222, 145 1992

[20] X. Shan and H. Chen, Simulation of non ideal gases and liquid-gas phase transitions by the lattice Boltzmann equation, Phys. Rev. E 49, 2941 – 2948, 1994.

[21] S. Chen, K. Diemer, G. Doolean, K. Eggert, C.Fu, S. Gutman and B. Travis, Lattice gas models for non ideal fluids, Physica D 47, 97, 1991

[22] A. A. Mohamad, Lattice Boltzmann method: fundamentals and engineering applications with computer codes, Springer Science & Business Media, (2011).

[23] P. Yuan, "Thermal lattice Boltzmann two-phase flow model for fluid dynamics," University of Pittsburgh, 2005.

[24] N. R. Koosukuntla, Towards development of a multiphase simulation model using Lattice Boltzmann Method (LBM), (2011**)**.

[25] D. Gao, Z. Chen, and L. Chen, A thermal lattice Boltzmann model for natural convection in porous media under local thermal non-equilibrium conditions, *International Journal of Heat and Mass Transfer* 70 (2014**)** 979-989.

[26] E. S. Boek and M. Venturoli, Lattice-Boltzmann studies of fluid flow in porous media with realistic rock geometries, *Computers & Mathematics with Applications* 59 (7) (2010**)** 2305-2314.

[27] Z. Guo and T. Zhao, Lattice Boltzmann simulation of natural convection with temperature-dependent viscosity in a porous cavity, *Progress in Computational Fluid Dynamics, an International Journal* 5 (1-2) (2004**)** 110-117.

[28] Z. Guo and T. Zhao, Lattice Boltzmann model for incompressible flows through porous media, *Physical Review E* 66 (3) (2002**)** 036304

[29] T. Seta, E. Takegoshi, and K. Okui, Lattice Boltzmann simulation of natural convection in porous media, *Mathematics and Computers in Simulation* 72 (2) (2006**)** 195-200.

[30] M. Jithin , Saurabh Siddharth , Malay K. Das , Ashoke De, Simulation of coupled heat and mass transport with reaction in PEM fuel cell cathode using lattice Boltzmann method, Thermal Science and Engineering Progress 4 (2017) 85–96

[31] A.ATIA ,Modeling and Simulation of Coupling Enhanced Oil/Gas Recovery with CO2 Injection, Thèse de Doctorat, Universite M'hamed Bougara-Boumerdes,2016

[32] M. Bayat, A. Abadi, and M. Jamialahmadi, The Application of the Lattice Boltzmann Method for Permeability Prediction of Porous Media: Investigating the Effects of Viscosity and Grid Resolution, *Petroleum science and technology* 30 (13) (2012**)** 1324-1334.

[33] T. Inamuro, M. Yoshino, H. Inoue, R. Mizuno, and F. Ogino, A lattice Boltzmann method for a binary miscible fluid mixture and its application to a heat-transfer problem, *J. Comput. Phys.* 179 (1) (2002**)** 201-215

[34] T. Seta, E. Takegoshi, and K. Okui, Lattice Boltzmann simulation of natural convection in porous media, *Mathematics and Computers in Simulation* 72 (2) (2006**)** 195-200.

[35] A. Mohamad, Lattice Boltzmann Method, Springer, (2011).

[36] F.Gao, B.Blunier, A.Miraoui, *Proton Exchange Membrane Fuel Cells Modeling*, Printed and bound in Great Britain by CPI Group (UK) Ltd., Croydon, Surrey CR0 4YY, 2012